EPA-600/2-78-032
February 1978

Environmental Protection Technology Series

EVALUATION OF THREE INDUSTRIAL PARTICULATE SCRUBBERS

Industrial Environmental Research Laboratory
Office of Research and Development
U.S. Environmental Protection Agency
Research Triangle Park, North Carolina 27711

EPA-600/2-78-032
February 1978

EVALUATION OF THREE INDUSTRIAL PARTICULATE SCRUBBERS

by

Seymour Calvert, Harry F. Barbarika,
and Gary M. Monahan

Air Pollution Technology, Inc.
4901 Morena Boulevard, Suite 402
San Diego, California 92117

Contract No. 68-02-1869
Program Element No. 1AB012
ROAP No. 21ADM-029

EPA Project Officer: Dale L. Harmon

Industrial Environmental Research Laboratory
Office of Energy, Minerals, and Industry
Research Triangle Park, N.C. 27711

Prepared for

U.S. ENVIRONMENTAL PROTECTION AGENCY
Office of Research and Development
Washington, D.C. 20460

RESEARCH REPORTING SERIES

Research reports of the Office of Research and Development, U.S. Environmental Protection Agency, have been grouped into nine series. These nine broad categories were established to facilitate further development and application of environmental technology. Elimination of traditional grouping was consciously planned to foster technology transfer and a maximum interface in related fields. The nine series are:

1. Environmental Health Effects Research
2. Environmental Protection Technology
3. Ecological Research
4. Environmental Monitoring
5. Socioeconomic Environmental Studies
6. Scientific and Technical Assessment Reports (STAR)
7. Interagency Energy-Environment Research and Development
8. "Special" Reports
9. Miscellaneous Reports

This report has been assigned to the ENVIRONMENTAL PROTECTION TECHNOLOGY series. This series describes research performed to develop and demonstrate instrumentation, equipment, and methodology to repair or prevent environmental degradation from point and non-point sources of pollution. This work provides the new or improved technology required for the control and treatment of pollution sources to meet environmental quality standards.

EPA REVIEW NOTICE

This report has been reviewed by the U.S. Environmental Protection Agency, and approved for publication. Approval does not signify that the contents necessarily reflect the views and policy of the Agency, nor does mention of trade names or commercial products constitute endorsement or recommendation for use.

This document is available to the public through the National Technical Information Service, Springfield, Virginia 22161.

ABSTRACT

Field measurements on three full scale industrial scrubbers were carried out to determine scrubber performance characteristics, including the particle collection efficiency as a function of particle diameter. The three scrubbers were different gas-atomized spray types with pressure drops ranging from 54 to 178 cm W.C. Their performance on major sources of fine particle emissions was compared to a mathematical performance model for venturi scrubbers.

CONTENTS

FIGURES

FIGURES (continued)

TABLES

TABLES (continued)

LIST OF ABBREVIATIONS AND SYMBOLS

A,B = parameters in equation (21) or equation (29), dimensionless

b = Weibull slope, dimensionless

B = venturi parameter (equation 5), dimensionless

C' = Cunningham slip correction factor (equation 9), dimensionless

CDF = cumulative distribution function, dimensionless

C_{Do} = drag coefficient at throat inlet, dimensionless

C_p = cumulative particle mass concentration, mg/DNm^3

C_{pti} = total inlet particle mass concentration, mg/DNm^3

C_{pto} = total outlet particle mass concentration, mg/DNm^3

$\overline{d}$ = differential operator

d_c = wire diameter of screen in screen diffusion battery, cm

d_d = drop diameter, cm or μm

d_j = jet diameter, cm

d_p = particle diameter, cm

d_{pa} = particle aerodynamic diameter, μmA

d_{pac} = impactor stage cut diameter, μmA

d_{pc} = diffusion battery stage cut diameter, cm

d_{pg} = particle geometric mass mean aerodynamic diameter, μmA

d_{pm} = particle mass median aerodynamic diameter, μmA

d_{pn} = particle geometric number (count) mean diameter, μm

d_{po} = Weibull minimum particle diameter, μmA

$f(d_p)$ = particle frequency distribution, dimensionless

K_p = inertial parameter equation (6) or equation (7), dimensionless

ℓ_t = venturi throat length, cm

m_p = mass of particles over a differential size element, g

N_p = cumulative number concentration of particles, $\#/cm^3$

P = cumulative mass fraction (equation 13), dimensionless

Pt = particle penetration, fraction

$\overline{Pt}$ = overall penetration, fraction or %

Q_G = gas volume flow rate, cm^3/s

Q_L = liquid volume flow rate, cm^3/s

S = solidity factor of screen diffusion battery stage, dimensionless

u_{de}^* = ratio of velocity attained by the liquid drops at the throat exit to the gas velocity, dimensionless

u_{Gt} = gas velocity in throat, cm/s

u_j = jet velocity, cm/s

u_s = superficial gas velocity, cm/s

x = length parameter (equation 3), dimensionless

x = parameter defined in equation (14), dimensionless

x,y = variables in equation (21), dimensionless

GREEK

ΔP = pressure drop, cm W.C.

O = Weibull characteristic particle diameter, μmA

μ_G = gas viscosity, poise (g/cm-s)

μmA = aerodynamic micrometers (equation 7)

ρ_p = particle density, g/cm^3

ρ_G = gas density, g/cm^3

ρ_L = liquid density, g/cm^3

σ_g = geometric standard deviation, dimensionless

ACKNOWLEDGEMENT

A.P.T., Inc. wishes to express its appreciation to Mr. Dale L. Harmon, the EPA project officer, for excellent coordination and assistance in support of our technical effort. The cooperation provided by the plant personnel at the sites tested is also greatly appreciated.

SECTION 1

INTRODUCTION

Air Pollution Technology, Inc. (A.P.T.) conducted performance evaluations on three industrial particulate scrubbers under EPA Contract No. 68-02-1869. The objective of the performance evaluations was to determine fine particle penetration as a function of particle size and scrubber parameters.

The project involved the following tasks:

1. Locate suitable scrubbers for evaluation and select those which:
   A. Have potential for high collection efficiency of fine particles,
   B. Control a process which is a major source of fine particulate emissions,
   C. Are widely used in industry.
2. Conduct appropriate field test programs to obtain necessary performance data.
3. Use data obtained to evaluate the performance and probable economics of the scrubber.
4. Develop a useful performance model of the scrubber system.

The first task involved an extensive correspondence campaign. Many leads were taken from listings in the National Emissions Data System (NEDS) and contacts with state and local air pollution control districts. The result of this task was the identification of the three scrubbers whose evaluations are presented in this report.

A separate detailed report has been issued for each of the scrubbers tested (Calvert, et al. 1976, Calvert, et al. 1977a, and 1977b). In this report each scrubber is discussed in a separate section and comparison with a performance model is made in a succeeding section. Also included in this report are discussions of the testing and the data reduction methods that were used.

SECTION 2

CONCLUSIONS

Field measurements on three full scale industrial scrubbers were conducted to determine scrubber performance characteristics, including the particle collection efficiency as a function of particle diameter. A summary of the performance tests is given in the tabulation below:

Control Device	Source	Pressure Drop cm W.C.
Variable Rod Venturi (National Dust Collector)	Iron Cupola	178
Venturi (American Air Filter)	Borax Fusing Furnace	110
Gas-atomized Spray Scrubber	Iron Cupola	54-104

All three scrubbers were in the general classification of gas atomized spray scrubbers and their performance was compared to the mathematical model of Yung, et al. (1977a).

The program achieved the primary objective of evaluating full scale industrial scrubbers, however some difficulty was encountered in finding suitable and willing facilities to evaluate. The following conclusions regarding venturi performance are based on the results of our evaluations.

1. Comparison of the measured particle collection efficiency to the mathematical model led to the following conclusions:
   (a) The comparison was good in the aerodynamic particle diameter region around 1 μmA.
   (b) In all cases the model predicted lower efficiency for particle diameters less than 0.5 μmA. To some extent this is expected because the model considers only inertial impaction as the collection mechanism.

(c) The comparison was not always good for particle diameters greater than 2 μmA. The model prediction in that size region was quite sensitive to the liquid-to-gas ratio, which usually was not known with precision. Thus the model may have been adequate in the range above 2 μmA, however knowledge of important variables was not precise and the adequacy of the model could not be fully proven.

(d) Predictions of overall efficiency were usually poor. The model, which assumed a log-normal size distribution, consistently underpredicted efficiency. Two probable reasons are that the inlet distribution had a geometric mass mean diameter greater than was measured with the heated cascade impactors and the size distribution was not log-normal.

Generally the model and the measured performance agreed. However, each source and scrubber had particular characteristics which requireed that some analysis be made to reconcile the model with the data. Therefore, the model should only be used with a full awareness of the assumptions on which it is based. The model may need modification if used in situations where conditions are significantly different from the assumptions in the model.

2. High pressure drop scrubbers are vulnerable to leaks which decrease the efficiency and waste power. Leaks generally develop because of improper construction materials and/or inadequate maintenance.

3. The cyclone entrainment separators used on the venturi and the gas-atomized spray scrubber were inefficient and caused both emissions problems and blower maintenance problems.

SECTION 3

NATIONAL DUST COLLECTOR MODEL 850 VARIABLE ROD MODULE VENTURI

SOURCE AND CONTROL SYSTEM

The emission source was an iron cupola which operated for ten hours per day. The cupola melted both the relatively clean ductile iron and the dirtier gray iron.

The primary component of the scrubbing system was a National Dust Collector Model 850 variable rod module venturi scrubber. The nominal capacity was 10.4 m^3/s at 21°C (22,000 CFM at 70°F). The variable rod module could be operated at pressure drops from 100 to 230 cm W.C. (40 to 90 inches W.C.). The venturi module consisted primarily of several parallel rods positioned normal to the gas flow. The gas was moved through the scrubber by two induced draft Buffalo No. 91 blowers used in series. Each blower, run by a 261 kW (350 HP) motor, was capable of drawing 114 cm W.C. (45 inches W.C.).

The overall scrubbing system is shown in Figure 1 . Gas flow from the cupola is controlled by adjusting the combustion (tuyere) air flow. The charge door is open so air continually leaks into the cupola. The temperature at the top of the cupola is only about 175-205°C instead of the much higher temperature encountered with most cupolas.

A series of quench sprays are introduced at the entrance of the connecting duct between the cupola tower and the scrubber. About 5.8 ℓ/s of fresh water is used in the quench section. The temperature of the gas is reduced to about 35°C by the quench sprays. The gas is saturated when it reaches the scrubber.

As shown in Figure 2 , the scrubber consists of the following sections:

1. A pre-spray section which sprays scrubbing liquor into the gas stream at the rate of 7.8 ℓ/s. This pre-spray has slight

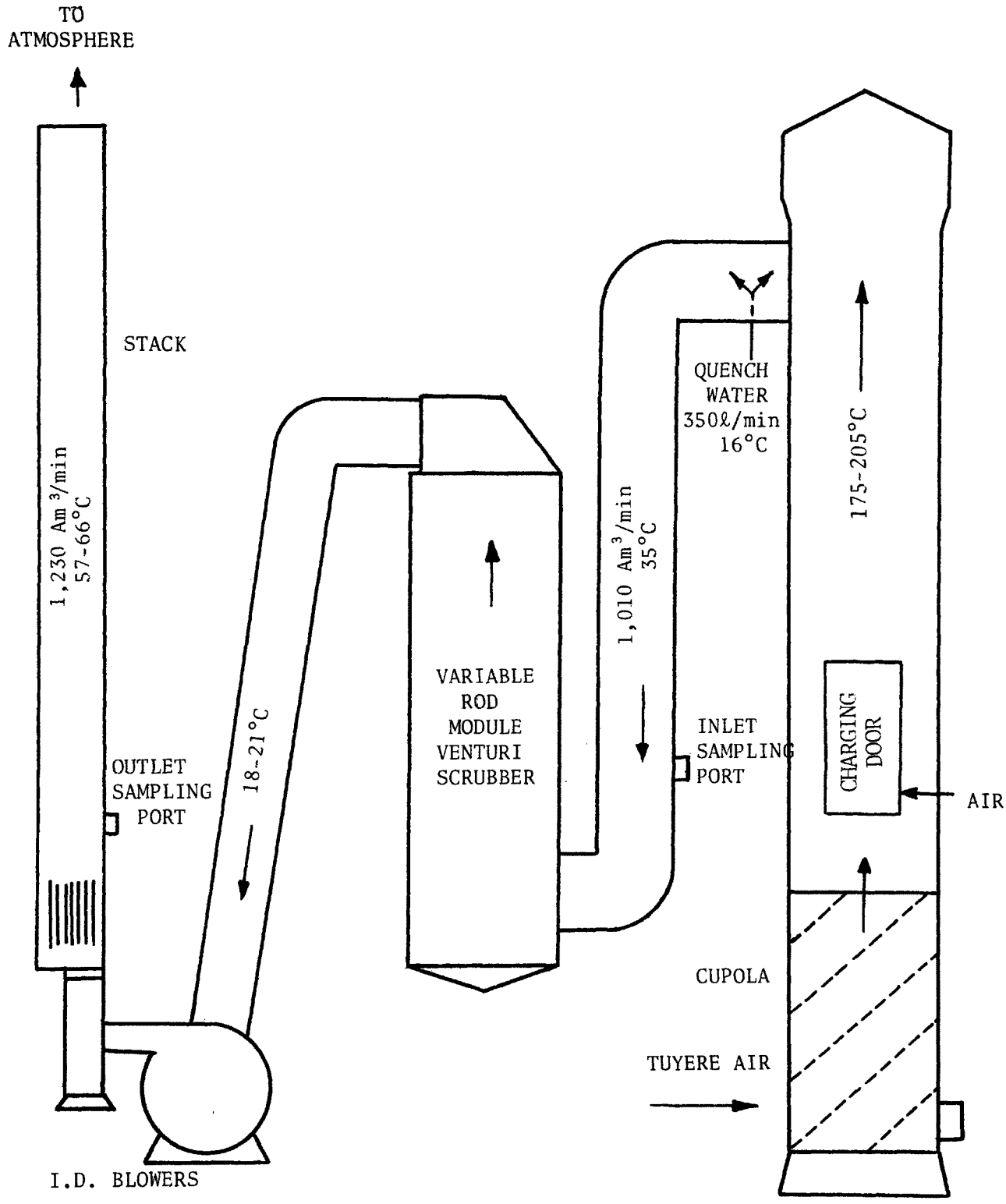

Figure 1. Schematic flow diagram of scrubbing system.

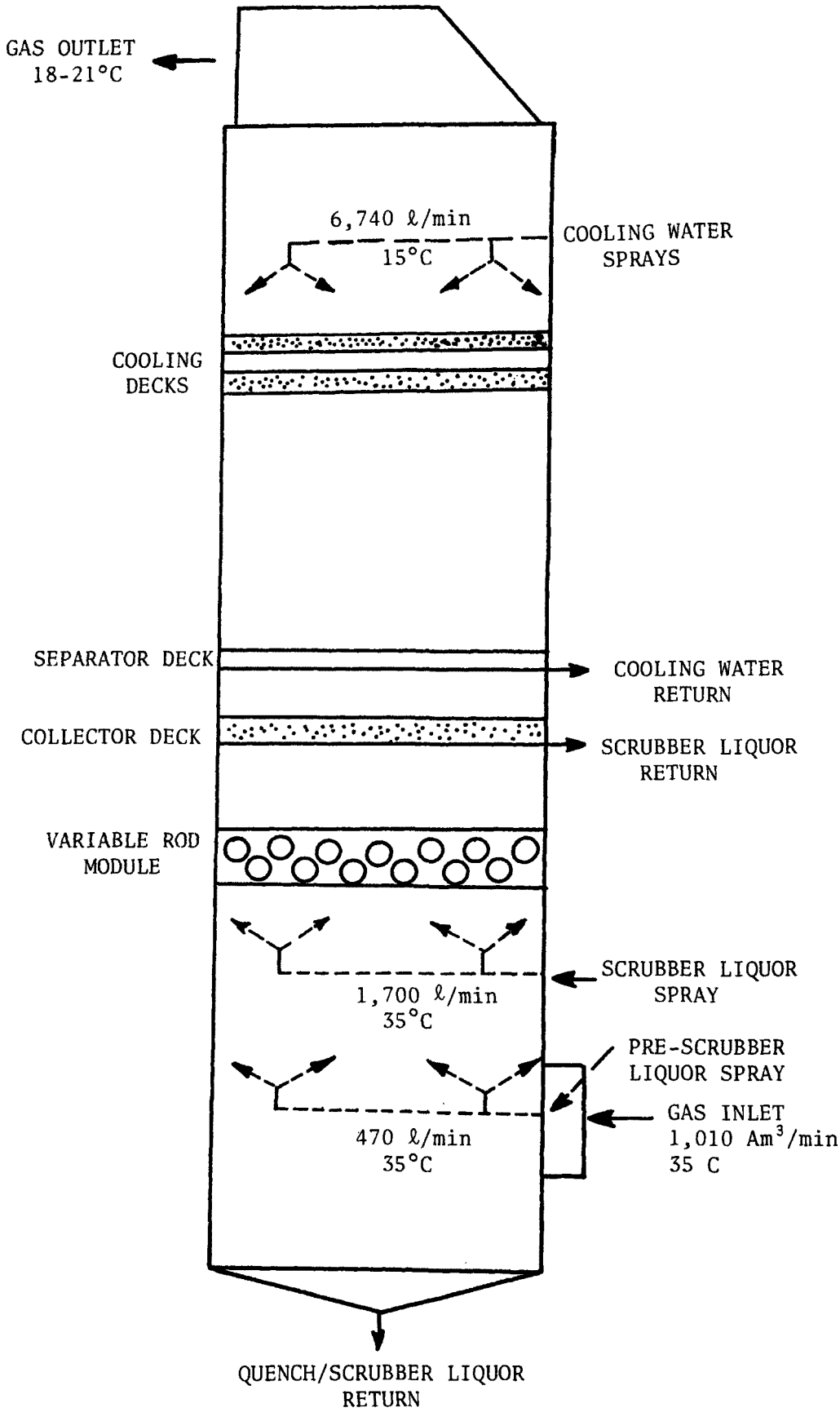

Figure 2. Schematic of scrubber tower.

cooling effect, which may cause some condensation growth of the particles, and it may collect some particles as it settles out onto the bottom of the scrubber tower. The drops from these sprays are not carried through to the variable rod module. The liquor returned from this section is sent to the sludge tank.

2. The high energy section, which consists of a scrubber liquor spray of 28.3 ℓ/s and the variable rod module is next. The pressure drop across the variable rod module is about 178 cm W.C. when the total pressure drop across the whole tower is 224 cm W.C. The temperature of the scrubber liquor is about 35°C and the ratio of liquid to gas volume flow rates in this section is about 1.68 ℓ/m^3.

3. The collector deck, consisting of 7.6 cm of loose 2.5 cm diameter marbles, separates out the entrained liquid from the high energy section. The returned scrubbing liquor is split into streams, with 80% going to the recycle tank and 20% going to the sludge tank.

4. Above the collector deck is a plate which collects the water from the cooling section.

5. The gas is cooled prior to leaving the scrubber tower in a cooling section consisting of sprays and two decks of single layer 2.5 cm diameter marbles. The cooling water is supplied at about 15°C at the rate of 112 ℓ/s to cool the gas to about 18-21°C. There is no carryover of entrainment from the cooling section.

PROCESS CONDITIONS

The operating conditions of the variable rod venturi scrubber for the period of sampling are shown below:

TABLE 1. PROCESS CONDITIONS

CONDITION	INLET SAMPLE PORT	OUTLET SAMPLE PORT (1)
Temperature	32-35°C	57-66°C
Velocity	9.2 m/s (30.3 fps)	25.3 m/s (83.1 fps)
Am^3/s	16.8	20.5
ACFM	35,700	43,500
DNm^3/s @ 0°C	12.9	14.5
DSCFM @ 21°C	27,300	30,800
Vol % H_2O Vapor	6.6	3.3
Static Pressure	-1.1 cm W.C.	+0.38 cm W.C.

Pressure Drop Across Tower	224 cm W.C.
Pressure Drop Across Venturi Module	178 cm W.C.
Superficial velocity Through Scrubber Tower (diameter 3.12 m) based on inlet ACFM	2.19 m/s

(1) The outlet sample port was located in the exit stack after the straightening vane section which was used to reduce the tangential spin of the gas. For this reason outlet flow rates may not be as reliable as inlet flow rates.

CASCADE IMPACTOR DATA

Sets of data were obtained from the variable rod module venturi scrubber as will be described later in the test method section. Fully developed flow enabled representative one-point sampling. Identical one-point sample locations were used for all the data points.

A summary of the inlet and outlet size distribution tests is given in Table 2. The distributions approached log-normality for diameters between 0.3 and 2 μmA.

Average sample times for the inlet were three to four minutes depending on the mass loading, while the outlet sample times averaged approximately forty-five minutes to one hour.

No inlet data were obtained for run 1 due to the excessive vacuum at the start of the run which overloaded the impactor.

Runs 9, 10, and 11 were not used as part of the data set because two of the five spray nozzles in the scrubber liquor spray section were disconnected while these runs were being made.

The data from the inlet cascade impactor runs was analyzed to determine the effect heating the impactors above the stack temperature had on the size distributions. We could see no definite trend in the heated impactor runs toward smaller size distributions than the unheated impactor runs.

DIFFUSION BATTERY DATA

Diffusion battery data were taken during the testing period. The runs were made alternately on inlet and outlet sample locations as shown in Table 3, while impactor runs were being performed.

Since operation of the scrubber was fairly constant over the testing period the inlet and outlet samples were averaged resulting in one set of data each for the ductile and gray operations.

TABLE 2. INLET AND OUTLET SIZE DISTRIBUTION SUMMARY USING LOG-PROBABILITY ANALYSIS

RUN NO.	OPERATION	INLET		OUTLET	
		d_{pg}, μmA	σ_g	d_{pg}, μmA	σ_g
1	Ductile	--	--	0.48	1.7
2	Ductile	0.69	2.0	0.52	1.8
3	Ductile	0.76	2.0	0.52	1.9
4(1)	Ductile	0.25	1.6	0.52	1.8
5	Ductile	0.27	1.5	0.56	1.8
6(2)	Gray	1.10	1.7	0.58	1.7
7(3)	Gray	1.51	1.8	0.56	1.8
8(4)	Gray	0.56	1.6	0.52	1.6
9(5)	Gray	0.54	1.5	0.63	1.6
10	Gray	0.62	1.6	0.63	1.7
11	Gray	1.90	1.6	0.81	1.7
12	Gray	0.62	1.6	0.51	1.6
13(6)	Gray	0.59	1.6	0.51	1.6
14	Gray	0.72	1.6	0.52	1.5
15(7)	Ductile	0.84	1.6	0.50	1.7
16	Ductile	0.58	1.5	0.48	1.7
16P	Ductile	0.71	1.7	0.48	1.7
17	Ductile	0.49	1.8	0.49	1.7

(1) Run 4 had 40% of the 5th stage holes plugged on the inlet sample
(2) Run 6 had 30% of the 3rd stage holes plugged on the inlet sample
(3) Run 7 had 30% of the 6th stage holes plugged on the inlet sample
(4) Run 8 had 20% of the 6th stage holes plugged on the inlet sample
(5) Run 9 had 30% of the 6th stage holes plugged on the inlet sample
(6) Run 13 had 4 holes of the 5th and 6th stages plugged on the inlet sample
(7) Run 15 had 50% of the 4th stage holes plugged on the inlet sample

TABLE 3. DIFFUSION BATTERY SIZE DISTRIBUTION ANALYSIS

Operation	Inlet		Outlet	
	$d_{pn,\mu m}$	σ_g	$d_{pn,\ \mu m}$	σ_g
Ductile	0.023	3.0	0.070	2.2
Gray	0.040	3.1	0.090	2.0

PARTICLE PENETRATIONS

Particle penetration versus particle aerodynamic diameter was computed and is shown in Figures 3 and 4 for ductile and gray iron operations respectively. Penetrations for a few of the runs are not shown because either their size distributions or their total loadings were outside a standard deviation from the mean of the set of data within which the run belonged.

The penetrations were calculated using a mathematical formula based on the log-normality of the inlet and outlet size distributions.

Diffusion battery data yield penetration related to physical size while cascade impactor data are in terms of aerodynamic size. In order to put the results on the same basis, it is necessary to know the particle density so that one can convert physical size to aerodynamic size (or vice versa). In Figures 3 and 4 a value of 3 g/cm^3 for density has been used to convert the physical diameter based on calculated diffusion battery penetrations to penetrations based on aerodynamic particle diameter.

The penetration plots indicate an increase in efficiency for particles smaller than 0.2 μmA. These results are consistent with published literature in that smaller, more highly diffused particles experience increased collection efficiency.

An overall penetration summary for runs 1 through 17 is presented in Table 4. Total inlet and outlet mass loadings were taken by cascade impactors.

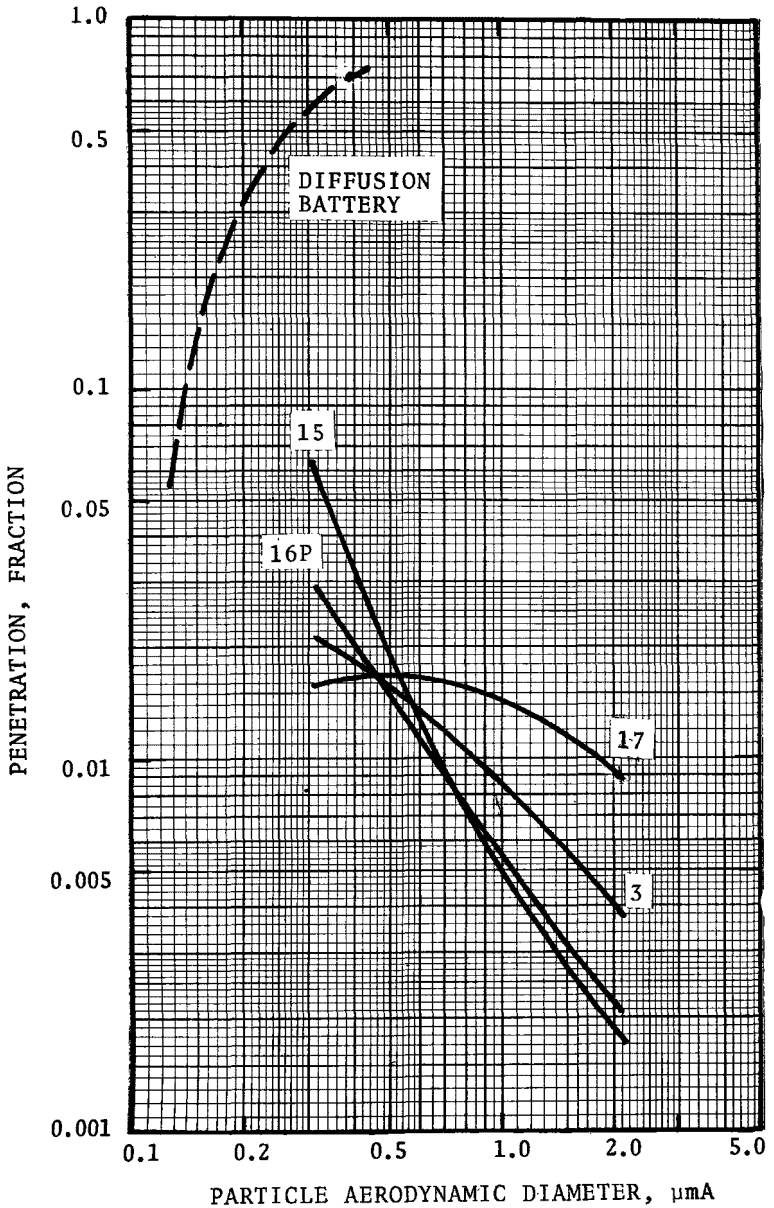

Figure 3. Penetration versus aerodynamic particle diameter for ductile operation.

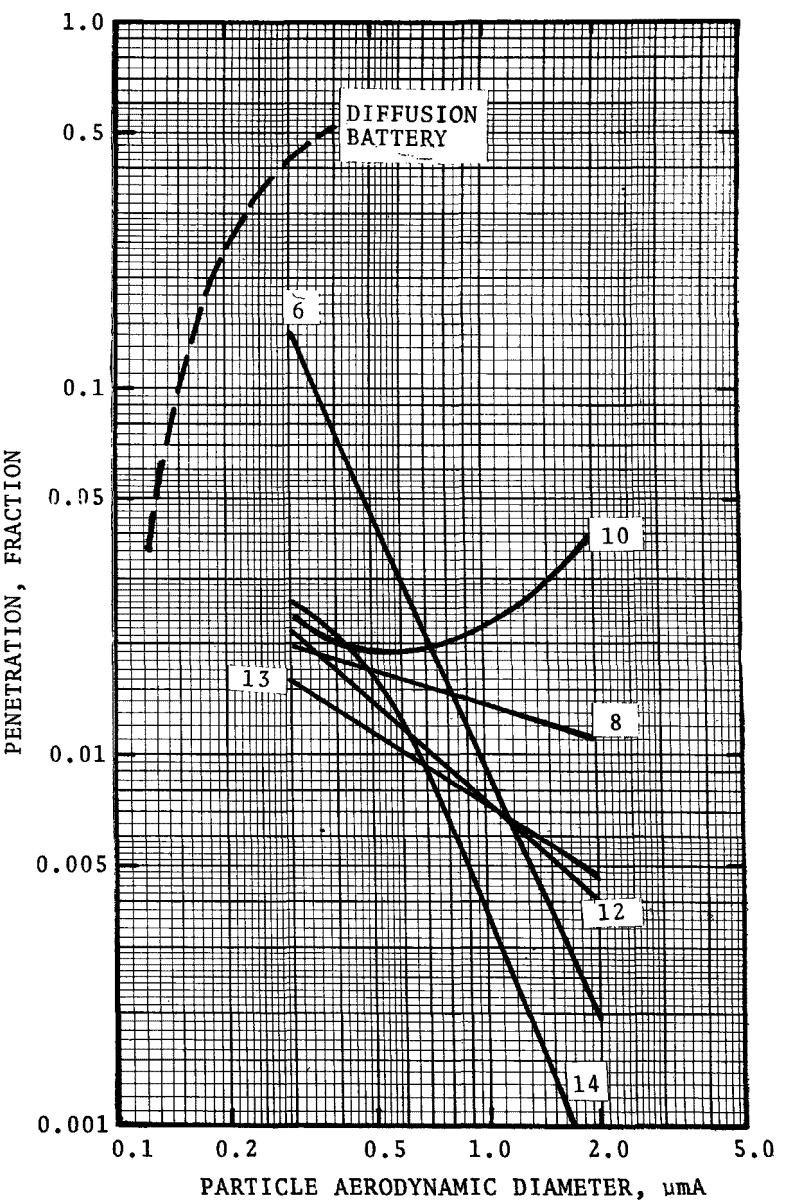

Figure 4. Penetration versus aerodynamic particle diameter for gray operation.

TABLE 4. OVERALL PENETRATION SUMMARY

RUN NO.	OPERATION (Gray) (Ductile)	MASS LOADING * mg/DNm^3		OVERALL, $\overline{Pt}$ %
		INLET	OUTLET	
1	D	---	23.6	---
2	D	2,050	20.9	1.02
3	D	2,100	24.5	1.17
4	D	1,430	28.0	1.96
5	D	1,810	27.0	1.49
6	G	2,060	32.0	1.55
7	G	1,910	30.7	1.61
8	G	2,230	35.8	1.61
9	G	2,310	58.5	2.53
10	G	1,880	39.3	2.09
11	G	2,100	52.9	2.51
12	G	2,290	27.9	1.22
13	G	2,260	24.0	1.06
14	G	2,320	23.0	0.99
15	D	1,960	21.2	1.08
16	D	1,790	24.8	1.39
16P	D	2,250	24.8	1.10
17	D	1,390	21.2	1.52

*N = 0°C, 1 atm

Although Figures 3 and 4 show penetrations for ductile and gray iron operations separately, there was no significant difference in the penetrations between the two operations. Likewise, the average overall penetration for both the ductile operations and the gray operation was 1.3%.

OPACITY

Opacity for the outlet stack of the National Dust Collector Model 850 variable rod module venturi scrubber was taken by employees trained and certified by the California State Air Quality Control Section. Readings were made five times a day from 8:00 a.m. to 4:00 p.m. every two hours.

A summary of the daily average reading is presented below in Table 5.

TABLE 5. OPACITY SUMMARY

Runs	Average Opacity, %
1	13
-	11
2,3	8
4,5	11
6,7,8	25
9,10,11	33
12,13,14	2
15,16,17	13
Average for Test	15

ECONOMICS

Cost data for the initial and annual cost was supplied by the user. The unit was originally built in 1967 as a fixed hole orifice venturi and in early 1975 was modified to a variable rod module type to alleviate plugging problems. Shown on Table 6 are the cost factors for the unit. F.O.B. shipping and delivery charges were not available, but should be about $15,000.

TABLE 6. COST DATA

Scrubber & Auxiliaries		
A. Fans, motors and motor starters		$136,200
B. Ducting		88,000
C. Liquid and solid handling and treatment		45,000
D. Instrumentation		7,800
E. Electrical material		55,000
	Total	$332,000
Scrubber Installation Cost		
A. Erection		$120,600
B. Plumbing		61,900
C. Electrical		36,000
D. Engineering		15,500
	Total	$234,000
Total Initial Cost (1967 prices)		$566,000
Annual Costs include the following factors:		
Operating Costs		
A. Utilities		$ 37,000
B. Labor		20,000
C. Supplies and materials		12,000
D. Treatment and disposal		4,000
	Total	$ 73,000
Maintenance Costs		
A. Labor		$ 10,000
B. Materials		6,000
	Total	$ 16,000
Plant overhead, space, heat, light, insurance		$ 7,000
Total Annual Costs		$ 96,000

SECTION 4

AMERICAN AIR FILTER KINPACTOR VENTURI

SOURCE AND CONTROL SYSTEM

The emission source was a large borax fusing furnace used in continuous operation. The furnace was capable of producing 270 metric tons per day of anhydrous borax ($Na_2B_4O_7$) from the penta-hydrated form of the feed, but was not always operating at full capacity during the testing. The particulates emitted were primarily the hydrated and anhydrous forms of borax which escaped during the drying and fusing processes.

The total scrubbing system is shown in Figure 5, with the location of the sampling ports indicated. The gases from the furnace at a temperature of 1,000°C to 1,100°C are quenched by scrubbing liquor to about 80°C. The gases then enter the American Air Filter Kinpactor 10 x 56 venturi scrubber. The venturi is rectangular in cross section with a throat height of 142 cm (56 inches). The throat width is automatically controlled to maintain a pressure drop of about 110 cm W.C. (43 in. W.C.) across the venturi. The throat width can vary from 0.64 cm (0.25 in.) to 25.4 cm (10 in.). Following the venturi the gases enter a cyclone entrainment separator. The gas is moved through the scrubbing system by a blower which is rated at 44 Am^3/s at 84°C and 114 cm W.C. pressure differential (93,500 ACFM, 184°F, 45 in. W.C.). The blower is powered by a 746 kW (1,000 HP) motor. The gases exhaust to the atmosphere through a 21 m tall, 2.13 m diameter stack.

The scrubbing liquor is recycled through a tank which is fed about 28 ℓ/s of fresh liquor or lesser amounts of fresh water. About 22 ℓ/s of concentrated liquor is pumped from the bottom of the tank so that the borax concentration of the liquor is maintained at from 10 to 15%.

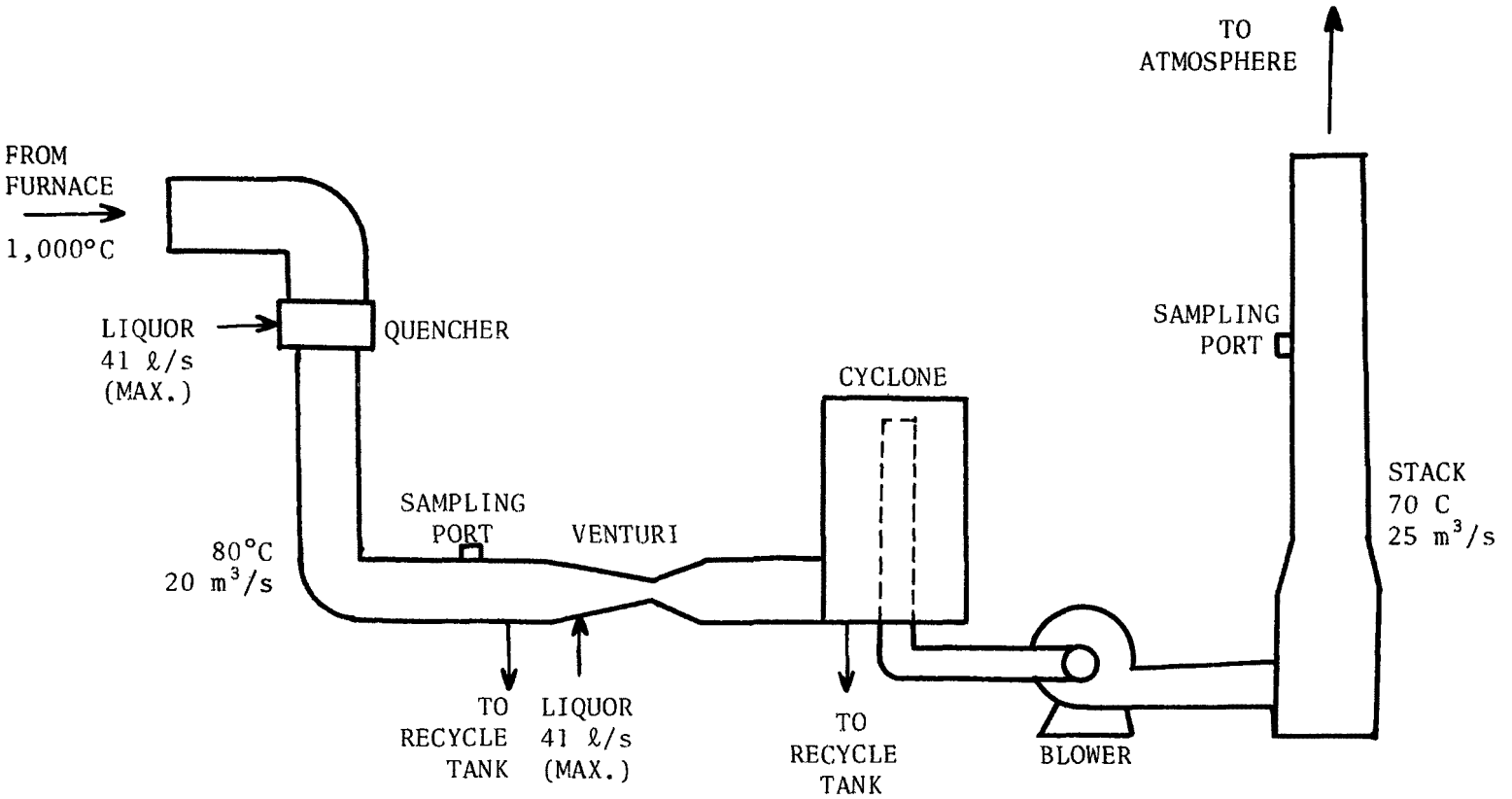

Figure 5. Schematic diagram of scrubbing system.

PROCESS CONDITIONS

The gas conditions at the inlet and outlet sampling locations for each run are presented in Tables 7 and 8. The conditions during runs 9 through 13 were thought to be most representative of normal conditions because of the amount and consistency of the product from the fusing furnace during these runs. The average barometric pressure during the testing period was 93.63 kN/m^2 (27.65 in. Hg).

Close examination of the inlet and outlet flow rates indicates a discrepancy in the measured flow rates. The outlet flow rate is greater than the inlet flow rate while the inlet temperature is greater than the outlet temperature. The static pressures are practically equal. There are two explanations for this flow rate discrepancy: (1) As noted previously, the inlet flow is not well developed and thus the inlet flow rate may not be accurate and, (2) air could be leaking into the system because of the low pressure (-110 cm W.C. gage) within the system between the venturi and the blower.

The results on the Orsat analysis of the outlet gas are presented in Table 9.

CASCADE IMPACTOR DATA

Particle size distribution data were obtained for the American Air Filter Kinpactor venturi scrubber as will be described in the test method section. Identical single point sampling at the average velocity location was performed at both the inlet and outlet. The sampling time of each run depended on the mass loading. The average sampling times for the inlet and outlet were nine and fifty minutes respectively.

Because of the number of very large particles in the inlet gas and the entrained water droplets at the inlet and outlet, precutters were used. The aerodynamic cut diameters of the inlet and outlet precutters were approximately 12 μmA and 4.5 μmA respectively. The inlet sampling was approximately isokinetic. However, because of the large amount of water droplets in the outlet gas, a special "rain can" had to be used on the outlet sampling nozzle.

TABLE 7 . INLET PROCESS CONDITIONS

Run	Temp. °C	Water Volume Percent*	Static Press. cm W.C.	Flow Rate Am^3/s (ACFM)
1	75	36	-8.3	24 (51,000)
2	108	57	-6.5	21 (45,000)
3,4,5	73	14	-6.1	16 (35,000)
6,7,8	78	23	-7.2	18 (38,000)
9,10,11	79	49	-7.5	20 (42,000)
12,13	81	41	-8.6	20 (43,000)

TABLE 8 . OUTLET PROCESS CONDITIONS

Run	Temp. °C	Water Volume Percent*	Static Press. cm W.C.	Flow Rate Am^3/s (ACFM)
1	80	31	-0.5	29 (62,500)
2	73	33	-0.4	25 (54,000)
3,4,5	72	38	-0.4	25 (54,000)
6,7,8	68	28	-0.4	25 (54,000)
9,10,11	71	23	-0.4	25 (53,000)
12,13	69	21	-0.4	25 (53,000)

*Based on wet and dry bulb temperatures

TABLE 9. OUTLET AVERAGE GAS COMPOSITION

Gas Component	Volume Percent (Wet)	Volume Percent (Dry)
N_2	60	85
O_2	6	8
CO_2	5	7
CO	0	0
H_2O	29	---
Molecular Wt.	26	29

Also, the outlet sampling nozzle was oriented perpendicular to the gas flow. The velocity through the outlet nozzle was maintained at the velocity of the outlet flow at that location.

To minimize the possibility of condensation in the impactors and to collect only the dry particles, the impactors were maintained at about 15°C above the gas stream temperature by using heating blankets. The precutters were not heated.

The fact that the impactors were heated should be noted when interpreting the size distribution data. Some unpublished data taken with heated and unheated cascade impactors in a stream of wet borax particles have shown differences in the size distributions. The primary difference was that the mass median aerodynamic diameter of the borax particles collected in heated impactors was as small as only 70% of the mass median aerodynamic diameter of the particles collected in unheated impactors. Thus, the venturi scrubber may be encountering larger aerodynamic size particles than the heated cascade impactor data indicate.

Data from run 3 are not included because the outlet cascade impactor stages had become wet. This happened because an attempt was made to sample with an outlet nozzle orientation parallel to the gas stream for this run.

Size Distributions

The inlet and outlet size distributions both seem to be bimodal. Thus, no attempt was made to fit all the data points to a log-normal curve. The size distributions were approximately log-normal in the region below 2 μmA. The mass mean geometric diameters and geometric standard deviations for the log-normal parameters as well as the mass median diameter (from the data points) runs are presented in Table 10.

Diffusion Battery Data

Diffusion battery data were taken during the fifth and sixth days of testing. The inlet data were taken during cascade impactor runs 9, 10 and 11, while the outlet data were taken during runs 12 and 13.

TABLE 10. PARTICLE SIZE DISTRIBUTION SUMMARY

Run	Inlet			Outlet		
	d_{pm}	d_{pg}	σ_g	d_{pm}	d_{pg}	σ_g
	μmA	μmA		μmA	μmA	
1	0.80	0.84	2.1	0.40	0.55	2.0
2	0.94	0.99	3.3	1.1	0.78	3.2
4	--	2.3	3.7	0.32	0.32	2.6
5	0.86	0.77	2.7	--	0.22	2.9
6	--	1.9	3.3	0.33	0.41	2.1
7	0.92	0.85	4.7	--	0.20	2.8
8	0.82	0.79	3.3	0.23	0.22	3.4
9	0.66	0.55	2.7	--	0.13	3.6
10	0.86	0.83	3.3	--	0.16	3.5
11	0.76	0.69	2.7	0.25	0.25	5.2
12	0.94	1.2	3.3	--	0.16	3.6
13	0.75	0.72	3.0	--	0.19	3.5

Note: d_{pm} = mass median aerodynamic particle diameter from data

d_{pg} = log-normal geometric mass mean aerodynamic particle diameter

σ_g = log-normal geometric standard deviation

Because of the large amount of water vapor (40% by volume) in the gas, the lenses in the condensation nuclei counter of the diffusion battery would fog when the diffusion battery was operated in the normal manner. Increased dilution did not solve the problem because the particle count would then drop below the threshold of the counter. Also, heating the diffusion battery to its maximum allowable temperature in an effort to reduce condensation on the lenses did not help.

The system was modified to allow data to be taken by routing the incoming source gas through a glass flask before entering the diffusion battery. Enough of the water vapor condensed in the flask so that the condensation nuclei counter did not become inoperable. Any condensation of water vapor would cause collection of submicron particles by diffusiophoresis. Thus, a fraction of the particles did not reach the diffusion battery. For this reason the diffusion battery data may not be accurate.

However, since the configurations for taking the outlet data and the inlet data were the same and the process was constant during the testing period, the data still give an indication of the relationship between the distribution of submicron particles at the inlet and outlet. The data show that the outlet submicron particles are larger and more monodisperse. This is an indication that particle growth by condensation may be occurring in the scrubber.

The data are only qualitative because condensation also occurred within the measuring system. However, mechanisms for particle growth are present in the scrubber system. These mechanisms are discussed later.

PARTICLE PENETRATIONS

Particle penetration versus particle aerodynamic diameter was calculated from the cascade impactor data. The results are shown in Figures 6 through 10 for each day of testing. Penetrations for run 1 are not shown because they are much larger than the penetrations for all the other runs, indicating anomalous

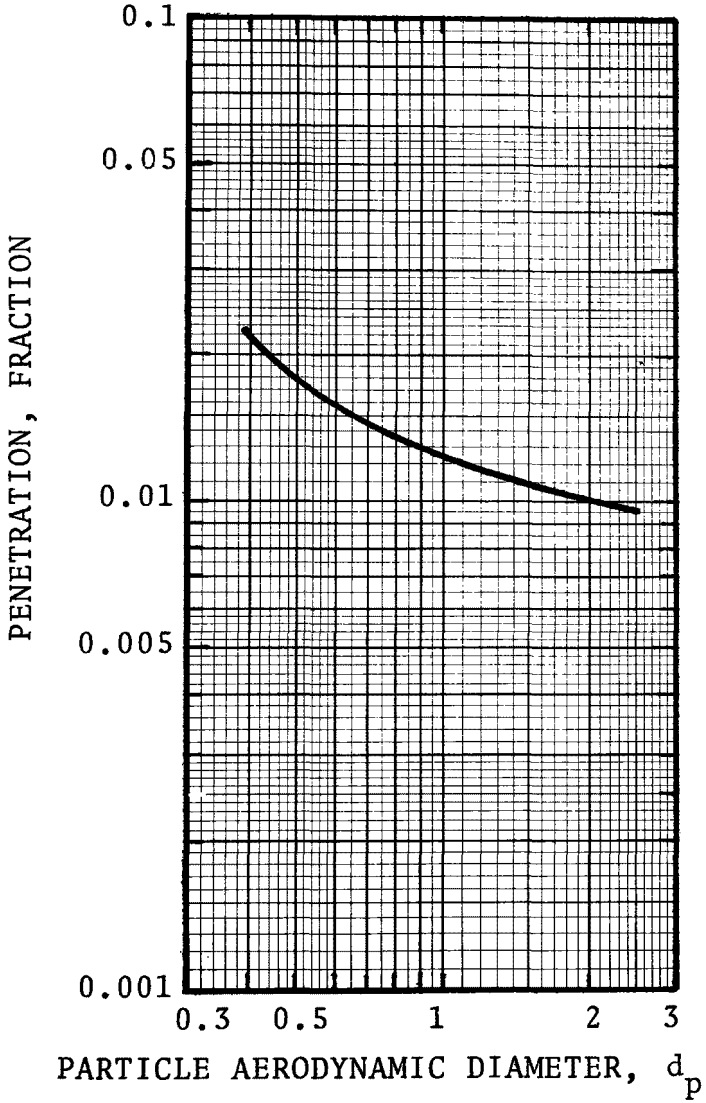

Figure 6. Particle penetration for run 2.

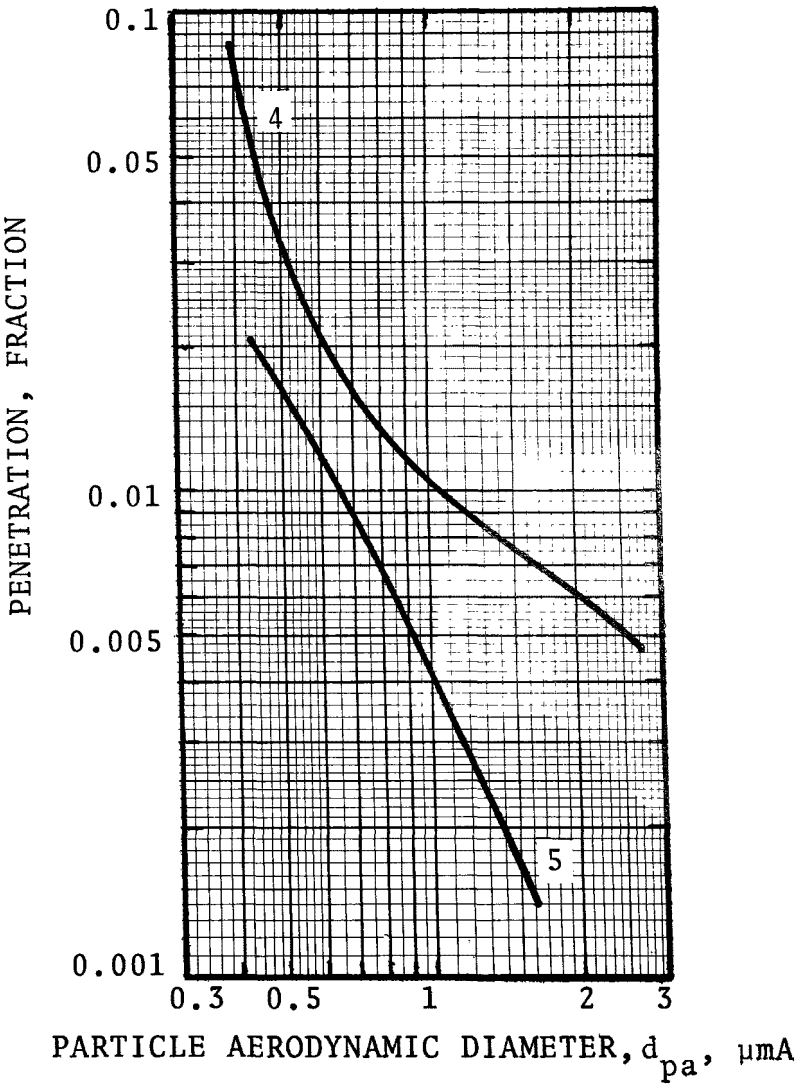

Figure 7. Particle penetration for runs 4 and 5.

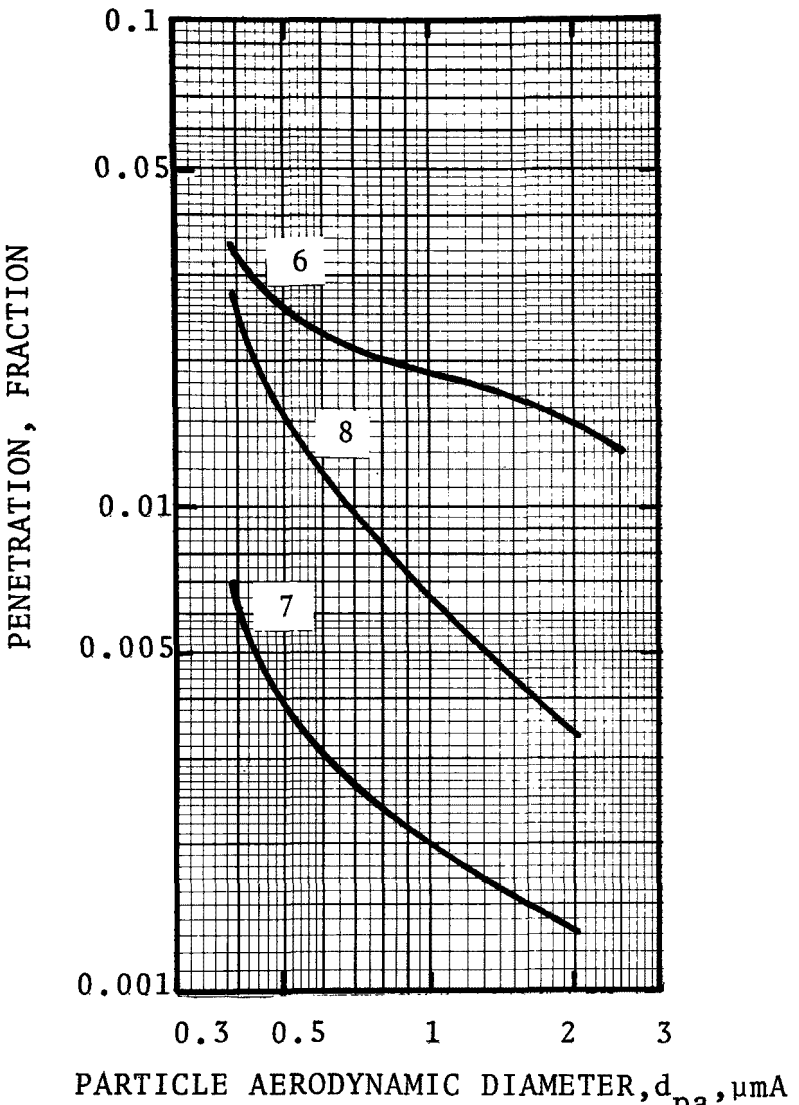

Figure 8. Particle penetration for runs 6, 7, and 8.

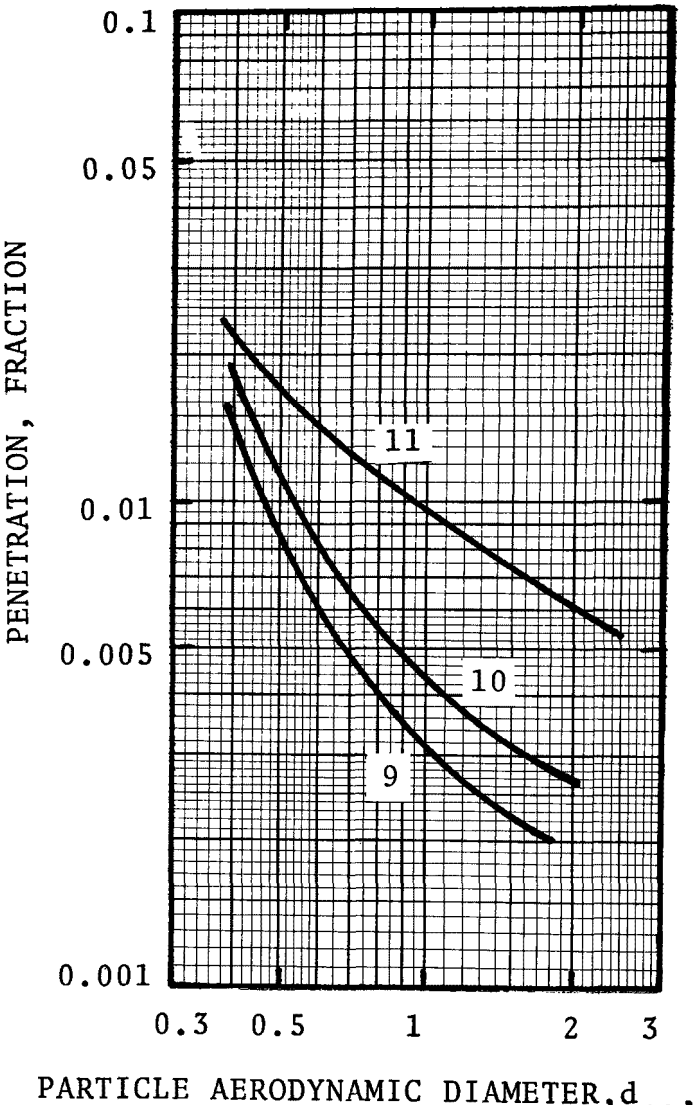

Figure 9. Particle penetration for runs 9, 10 and 11.

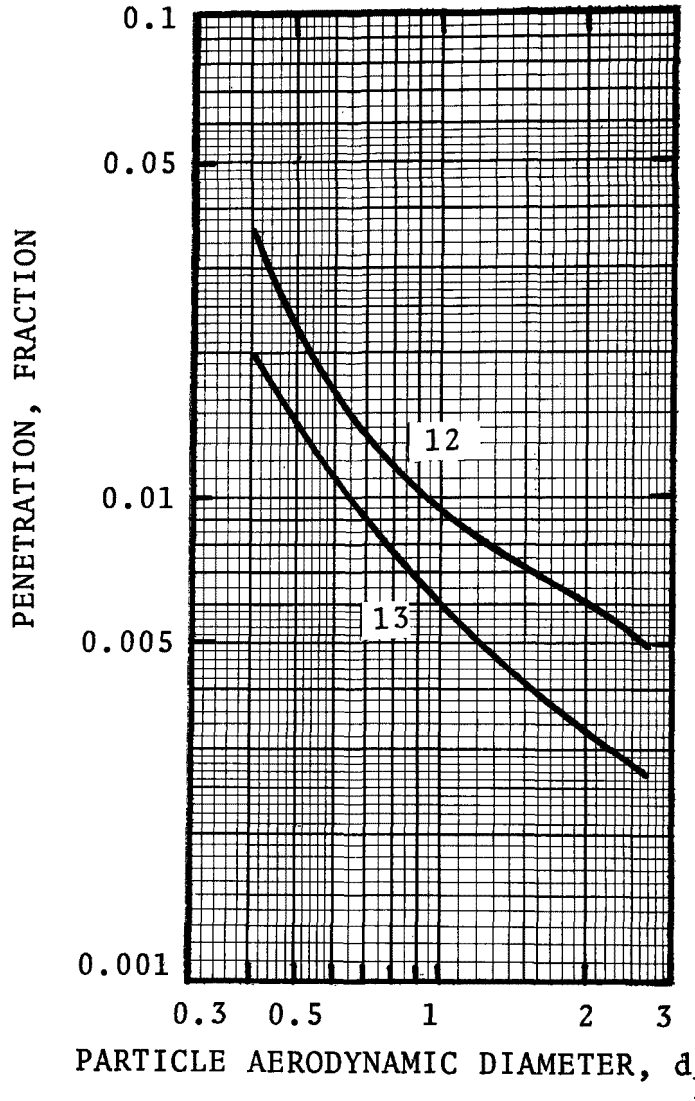

Figure 10. Particle penetrations for runs 12 and 13.

behavior. Penetrations for runs from the last two days, when operations were most smooth, are quite consistent.

Because the size distributions were not log-normal all of the penetrations were calculated manually. Particle penetration based on diffusion battery data is not presented because of the inaccuracies incurred during the data acquisition. Diffusion battery data are discussed in the previous section.

The total mass loadings and overall penetrations for the runs are presented in Table 11. The total mass loading was determined from analysis of the cascade impactor data. Run 1 had anomalously high overall penetration and high flow rates which indicated that something may have been wrong with the data or that the venturi was not operating properly during that run. The average penetration for all of the runs, exclusive of run 1, was 2.5%.

TABLE 11. MASS LOADING AND OVERALL PENETRATION

Run	Inlet Mass Loading mg/DNm^3	Outlet Mass Loading mg/DNm^3	Penetration %
1	332	40.4	12.2
2	653	18.3	2.8
4	1,150	42.1	3.7
5	841	11.0	1.3
6	690	21.9	3.2
7	2,310	18.4	0.8
8	882	20.5	2.3
9	829	22.7	2.7
10	1,040	19.3	1.9
11	863	31.0	3.6
12	1,210	36.9	3.0
13	1,000	27.3	2.7

OPACITY

Opacity for the outlet stack of the American Air Filter Kinpactor 10 x 56 venturi scrubber was determined by personnel trained and certified by the California Air Resources Board. Readings were made hourly during the testing period. The opacity determinations were made somewhat difficult by the presence of steam condensation in the plume and the proximity of other stacks emitting similar particulates.

Table 12 presents the daily average opacity readings.

TABLE 12. OPACITY

Date	Runs	Average Opacity, %	Average Outlet Loading, mg/m
8/19/76	2	10-15	9
8/20/76	3-5	15	12
8/21/76	6-8	20	11
8/22/76	9-11	15-20	14
8/23/76	12,13	20	19

ECONOMICS

Data for the initial costs of the venturi-cyclone scrubbing system, purchased in 1970, were supplied by the user:

Approximate scrubber purchase cost	$200,000
Scrubber auxiliaries:	
1. Fans, motors, etc.	30,000
2. Ducting	47,000
3. Liquid and solid handling and treatment	50,000
4. Instrumentation	45,000
5. Electrical material	36,000
Scrubber installation:	
1. Site preparation	108,000
2. Installation	100,000
3. Startup and modification	51,000
4. Engineering	63,000
Total Initial Cost -	$730,000

The operating costs were not available. However, the power costs can be estimated. The major power user is the large blower. The blower is powered by a 746 kW (1,000 HP) motor. At $0.03 per kW-hour the fan power would cost $22 per hour, or $537 per day.

OPERATING PROBLEMS

The primary operating problems with the system are the plugging of nozzles ~~and~~ piping and scale build-up in the system. These problems are all caused by calcium carbonate and sulfate deposits. The local water is very hard and the feed to the fusing furnaces may also contain these mineral impurities. To combat this problem special reamer nozzles have to be used and the system has to be shut down periodically to chip away the built-up scale.

Although a large amount of entrained water was carried-over from the entrainment separator through the fan, and out the stack, it was not considered a problem by operating personnel.

SECTION 5

GAS-ATOMIZED SPRAY SCRUBBER

SOURCE AND CONTROL SYSTEM

The emission source for this test was a no. 7 gray iron cupola used for an 8 to 9 hour/day operation. The cupola normally is run for 3 days/week, but during the test period it was run for as many days as possible (3 days in the first week, 5 days in the second week). The operation produces 10 to 12 tons per hour of metal from a feed of scrap metal, coke, and limestone.

During the testing period the cupola ran at normal conditions. The particulate emissions result from the melting of the scrap and burning of the coke in the cupola. Figure 11 is a schematic diagram of the entire operation including the scrubber system.

The hot gases from the melting operation enter the afterburner where it reaches approximately 700 - 1,000°C. The gas is then quenched by city water, which during the test had a flow rate varying between 0 and 2.6 ℓ/s (4.1 GPM) giving a temperature range of 700°C to 60°C. Scrubber liquor is added just ahead of the throat section (the rate was varied during the testing period from 2.5 ℓ/s to 15.8 ℓ/s). Next the gas enters a variable throat scrubber section which is a rectangularly cross-sectioned orifice with a throat height of 91.4 cm (36 inches). The throat width can be varied from 4.2 cm (1.7 in.) to 11.4 cm (4.5 in.). Following the venturi the gas enters a cyclone type entrainment separator. An induced draft blower moves the gas through the scrubbing system, powered by a 298 kW (400 HP) motor. From this blower the gas is exhausted through an 11.9 m (39 ft) high, 0.91 m (3 ft) diameter stack.

At the venturi section, scrubber liquor is pumped in through pipes placed directly upstream of the throat. This liquor

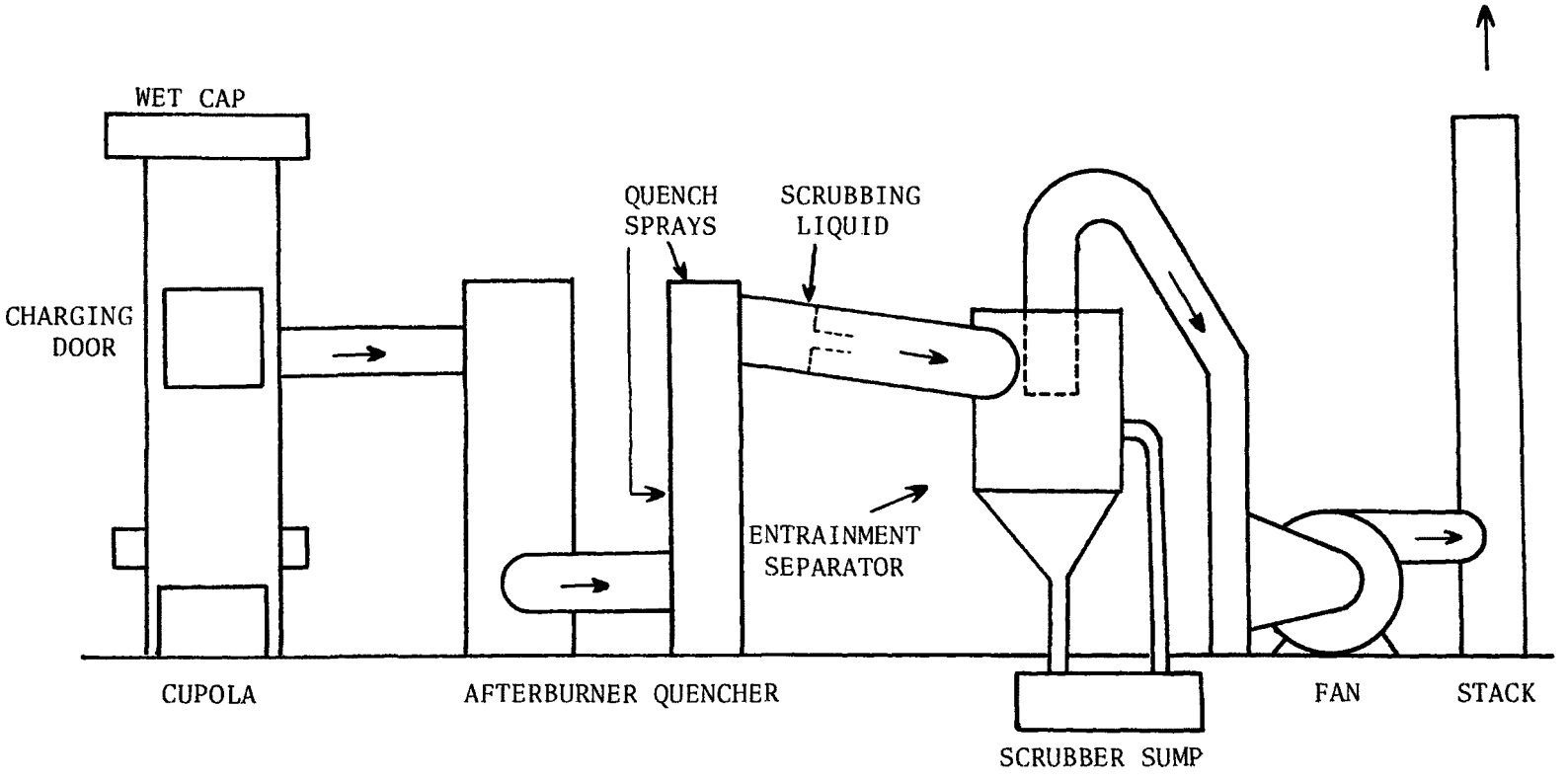

Figure 11. Schematic drawing of scrubber system.

begins as clean water every day from a sump below the cyclone. No fresh water feed is added to this liquor so that as the day progresses the solids concentration increases. When the system is shut down the sump is neutralized, cleaned out, and fresh water pumped in for the next day of operation.

The water used for the quench sprays, however, comes directly from the city water lines and no recirculation is used.

PROCESS CONDITIONS

The scrubber process conditions for the inlet and the outlet are shown in Tables 13 and 14 . Runs 1 through 4 represent the scrubber running with a number of leaks, as can be seen by comparing the inlet and outlet flow rates. Between runs 4 and 5 many of the large leaks were patched, resulting in much smoother operation as well as a reduction of the fan amperage, an increase in the inlet flow rate, and reduction in the outlet flow rate.

After patching most of the leaks, more control over the scrubber operation could be maintained. It was then possible to adjust water flow rates as well as the pressure drop across the venturi. This enabled a number of test conditions to be examined. For the most part, the charging operation was fairly constant and did not vary significantly between the runs, except for run 1 when the crane broke and only one charge was added during the entire run. The average barometric pressure during the testing period was 99.36 kPa (29.34 in. Hg).

The top of the cupola was open, except for a "wet cap." The wet cap consists of baffles and sprays at the top of the cupola and it was operated during the test period. Depending upon the scrubber conditions, varying quantities of visible emission were observed flowing from the wet cap.

The tests were conducted during the winter so that the ambient temperature averaged about 0°C during the testing. This low ambient temperature probably caused the temperature of the gases entering the scrubber to be lower than normal because of heat transfer through duct walls, leakage of cold air, and use of cooler than normal quencher and scrubber water.

TABLE 13. SCRUBBER CONDITIONS

Run No.	P_1 *	P_2 *	ΔP *	Throat Width (cm)	Scrubber Liq.Flow (ℓ/s)	Quench Flow (ℓ/s)
1	-1.8	- 77.5	75.7	11.4	3.2	1.1
2	-1.3	- 81.3	80.0	4.4	11.4	0.0
3	-3.0	- 57.2	54.2	5.6	< 2.5	1.6
4	-2.0	- 64.8	62.8	4.4	< 2.5	1.6
5	-6.4	- 83.8	76.4	11.4	12.6	1.6
6	-6.4	- 85.1	78.7	11.4	12.6	1.6
1-B	-6.6	- 87.6	81.0	11.4	12.6	1.6
7	-6.1	- 87.6	81.5	11.4	12.6	1.6
8	-3.8	- 86.4	82.6	5.1	9.5	1.6
2-B	-3.6	- 85.1	81.5	5.1	9.5	1.6
9	-5.1	- 87.6	82.5	5.6	9.5	0.0
10	-4.3	- 85.1	80.8	5.6	9.5	0.0
11	-2.3	-105.0	103.0	4.2	12.6	2.6
12	-2.5	-105.0	104.0	4.3	12.6	2.5
13	-2.8	-107.0	104.0	4.3	12.6	2.5
14	-5.8	- 94.0	88.2	11.4	15.8	1.7
15	-5.8	- 92.7	86.9	11.4	15.8	1.7

P_1 = static pressure before venturi
P_2 = static pressure after venturi
$\Delta P = P_1 - P_2$
* = numbers expressed in cm W.C.

TABLE 14. PROCESS CONDITIONS

Run No.	Inlet Temp. °C	Outlet Temp. °C	Inlet Water Vapor Vol.%	Outlet Water Vapor Vol.% **	Inlet Flow Rate Am /s (MACFM)	Outlet Flow Rate Am /s (MACFM) ***
1	246	56	21	7	5.2(11.0)	11.7(24.8)
2	496	56	11(6*)	7	6.2(13.2)	11.7(24.8)
3	132	57	27	17	6.5(13.7)	12.5(26.5)
4	132	57	27	17	6.5(13.7)	12.5(26.5)
5	177	65	25	20	11.4(24.1)	10.5(22.2)
6	149	65	26	20	11.0(23.4)	10.5(22.2)
1-B	149	65	26	20	11.0(23.4)	10.5(22.2)
7	177	54	25	5	10.8(22.9)	10.0(21.1)
8	177	54	25	5	10.8(22.9)	10.0(21.1)
2-B	177	54	25	5	10.8(22.9)	10.0(21.1)
9	699	58	2*	5	12.6(26.7)	8.1(17.1)
10	677	58	2*	5	12.5(26.4)	8.1(17.1)
11	68	51	27	8	4.1(8.7)	7.0(14.8)
12	60	51	20	8	4.0(8.4)	7.0(14.8)
13	71	51	32	8	4.2(8.8)	7.0(14.8)
14	66	51	25	11	9.1(19.2)	9.8(20.7)
15	177	51	25	11	10.4(22.2)	9.8(20.7)

* Based on sampling train water catch
** Based on wet and dry bulb temperatures
*** MACFM = thousand actual cu. ft/min

The cyclone separator was not operating efficiently during the testing period. It was patched along with the rest of the system after run 4 but it could not be sealed completely as it had been repeatedly patched previously. Any leakage into the cyclone would disrupt the flow of liquid down the walls and would cause reentrainment. Entrainment emission was clearly noticeable as rainout from the stack. The entrainment emission was due to several factors such as leakage, poor flow distribution at the inlet, and internal roughness due to scale buildup.

The Orsat analyses of the outlet gases are presented in Table 15.

CASCADE IMPACTOR DATA

Particle size distribution data were obtained for the gas-atomized spray scrubber as described in the test method section. Identical single point sampling at the average velocity location was performed at both the inlet and outlet. The sampling time for each run depended upon the mass loading. The average sampling times for the inlet and outlet, respectively, were 6.5 and 31 minutes.

The inlet sample ports, because of a limited length of ducting after quencher and before the venturi throat, were located 0.73 equivalent duct diameters downstream of a 78° bend and 0.73 equivalent duct diameters from the beginning of the venturi section. The inlet duct was rectangular (0.91 m x 0.61 m) and its equivalent duct diameter was 0.73 m as calculated by EPA Method 1.

The outlet sample ports were located in a 0.91 m (3 ft) diameter round stack, about 8 stack diameters downstream of the inlet from the fan and 3 diameters upstream of the stack air. The velocity traverses indicated a well-developed flow pattern.

Entrained water drops were a problem at both the inlet and outlet, so precutters for the inlet and outlet were approximately 11.6 μmA and 5.6 μmA, respectively. Both the inlet and outlet sampling were approximately isokinetic.

To minimize the possibility of condensation in the outlet

TABLE 15. AVERAGE GAS COMPOSITION

Gas Component	Inlet Volume,% Dry	Outlet Volume,% Dry (Runs 1-4)	Outlet Volume,% Dry (Runs 5-15)
N_2	80.1	80.1	79.6
O_2	6.4	16.9	14.6
CO_2	13.2	3.0	5.8
CO	0.3	0	0
Molecular Wt.	29.9	28.8	29.2

impactors and to collect dry particles, the impactors (except run 9 which was below the stack temperature due to a malfunction of the heating blanket) were maintained at about 13.5°C above the gas stream temperature using heating blankets. Because of the temperature fluctuation at the inlet the impactor was kept out of the stack and heated by a heating blanket to an average temperature of 86°C. In both cases (inlet and outlet) the precutters were not heated.

The fact that the impactors were heated should be remembered when interpreting the size distribution data. Because of the presence of a quencher upstream of the scrubber section, the particles may be wet due to condensed or absorbed water when they enter the scrubber. The wet particles would have a different size distribution than those collected in a heated impactor. The wet particle size distribution would probably have a larger mass median diameter. The runs with the most favorable conditions for wet particles were runs 11-14.

Table 16 summarizes the "d_{pg}" and "σ_g" results for the cascade impactor runs using log-probability parameters. The distribution data include only the results of the cascade impactor stage analysis. The precutter and probe weight gains were not used. The log-normality approximation was adequate only for diameters between 0.2 and 2 μmA.

DIFFUSION BATTERY DATA

Diffusion battery data were taken during cascade impactor runs as shown in Table 17.

A dilution system was used for this testing along with the A.P.T. diffusion battery. A 208 liter (55 gallon) drum was used upstream of the diffusion battery as the dilution system. Samples were not taken continuously from the stack because the intermittent charging operation can result in rapidly changing readings. A syringe was inserted into the stack several times to withdraw gas samples and these were expelled into the dilution tank. Later this system was switched to a calibrated hand pump. These gas samples were diluted with dry filtered air

TABLE 16. CASCADE IMPACTOR DATA USING LOG-PROBABILITY ANALYSIS

Run No.	Inlet d_{pg} (μmA)	Inlet σ_g	Outlet d_{pg} (μmA)	Outlet σ_g
1	0.47	2.6	0.86	1.9
2	0.45	2.9	0.76	4.0
3	0.40	2.1	0.38	2.3
4	0.26	2.7	0.58	2.3
5	0.19	3.4	0.36	2.3
6	0.33	2.0	0.43	2.2
7	0.39	2.0	0.41	2.2
8	0.45	2.0	0.39	2.5
9	0.58	2.0	0.49	2.3
10	0.37	2.7	0.35	2.7
11	0.40	2.4	0.53	2.0
12	0.41	2.4	0.43	2.7
13	0.31	2.7	0.41	2.4
14	0.20	4.4	0.43	2.4
15	0.18	4.4	0.49	2.2

TABLE 17. DIFFUSION BATTERY PARTICLE SIZE DISTRIBUTIONS

D.B. Run No.	Impactor Run No.	Type of Run	d_{pn} (μm)	σ_g	Total Particle Count** No./cm^3
3	5	In	0.070	3.4	9.0×10^6
4	5	In	0.092	12.0	1.1×10^7
5	6	In	0.095	12.0	1.1×10^7
6	1-B	In	0.128	14.0	3.9×10^6
7	8	In	0.072	6.0	2.3×10^6
8	8	In	0.095	2.9	1.3×10^6
9	2-B	In	0.094	11.5	1.1×10^7
10	2-B*	Out	0.057	1.0	5.1×10^6
11	2-B*	Out	0.061	2.5	8.0×10^6
12	2-B*	Out	0.085	4.5	8.3×10^5
13	11	Out	0.090	6.0	7.8×10^5
14	11	Out	0.090	8.9	1.9×10^6
15	12	In	0.086	9.3	2.2×10^7
16	13	In	0.059	6.0	1.5×10^7

*Same condition but not simultaneous

**Gas conditions: 20°C, 1 atm

in the tank and run through the diffusion battery with particle counts being measured using the condensation nuclei counter.

The particle size distributions determined by diffusion battery analysis are given in Table 17.

PARTICLE PENETRATIONS

Particle penetrations for various particle aerodynamic diameters were calculated from cascade impactor and diffusion battery cumulative loading data. The penetrations based on diffusion battery data were calculated from log-normal inlet and outlet cumulative distributions. The physical (actual) size distributions from the diffusion battery analysis were converted to aerodynamic size by assuming the cupola dust had a particle density of 2.5 g/cm^3.

Since the size distributions were not log-normal, the cascade impactor penetrations presented in Figures 12 through 18 were calculated graphically.

The total mass loadings and overall penetration for the runs are presented in Table 18. Mass loading and penetration are also shown without the outlet precutter catch. The reason is that the precutter loading was mostly entrainment carryover from the cyclone and was not due to scrubber inefficiency.

TABLE 18. MASS LOADING AND OVERALL PENETRATION

Run No.	Mass Loading, mg/DNm *			Penetration, %	
	Inlet	Outlet[1]	Outlet[2]	Pt[1]	Pt[2]
1	1,570	212	46.3	13.5	2.9
2	2,120	74.3	36.5	3.5	1.7
3	1,100	280	267	25.5	24.4
4	2,060	176	175	8.5	8.5
5	3,190	609	514	19.1	16.1
6	2,340	341	307	14.6	13.1
1-B	7,030	968	-	13.8	-
7	2,530	234	234	9.3	9.2
8	1,913	320	98.2	16.7	5.1
2-B	1,600	177	-	11.1	-
9	5,070	198	156	3.9	3.1
10	2,620	589	159	22.5	6.1
11	1,750	159	153	9.1	8.7
12	2,370	214	159	9.0	6.7
13	2,500	797	174	31.8	6.9
14	1,450	278	186	19.2	12.8
15	1,240	277	223	22.2	17.9

[1] Including outlet precutter dry weight gain

[2] Without outlet precutter dry weight gain

* N = 0°C, 1 atm

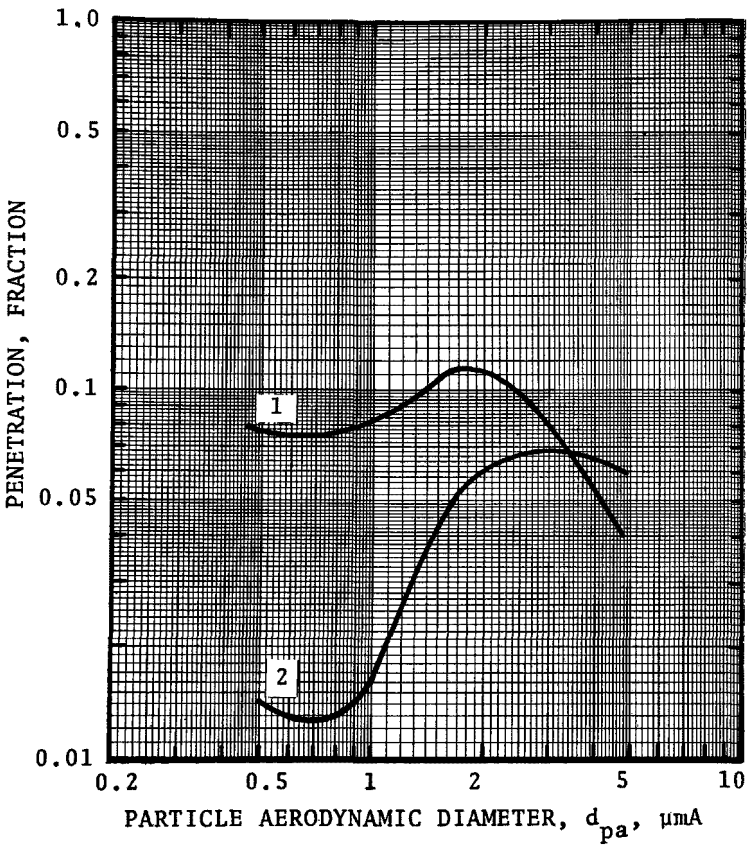

Figure 12. Particle penetration for cascade impactor runs 1 and 2.

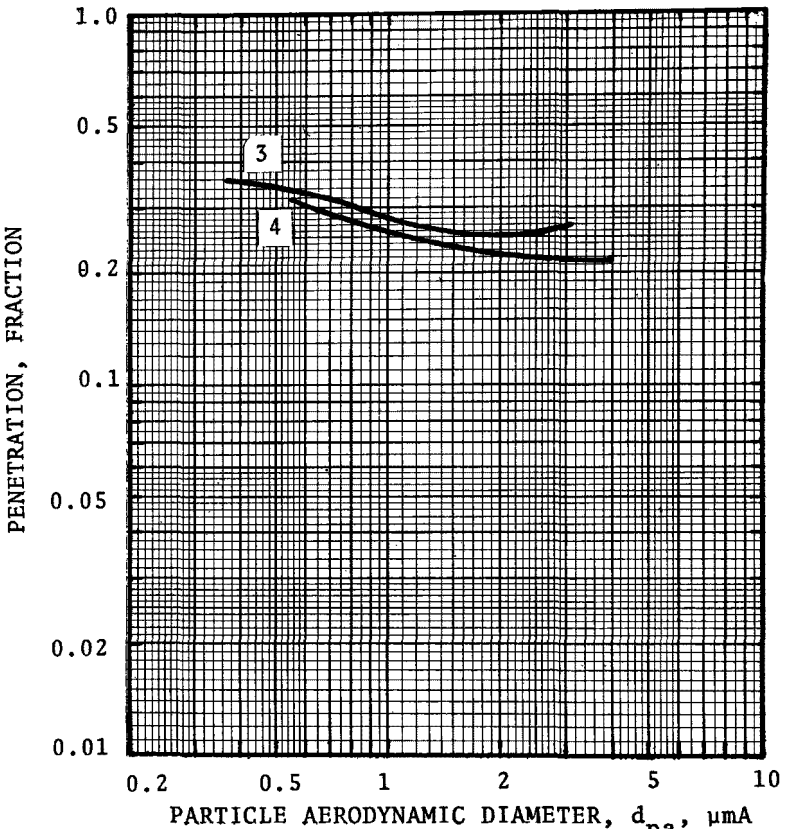

Figure 13. Particle penetration for cascade impactor runs 3 and 4.

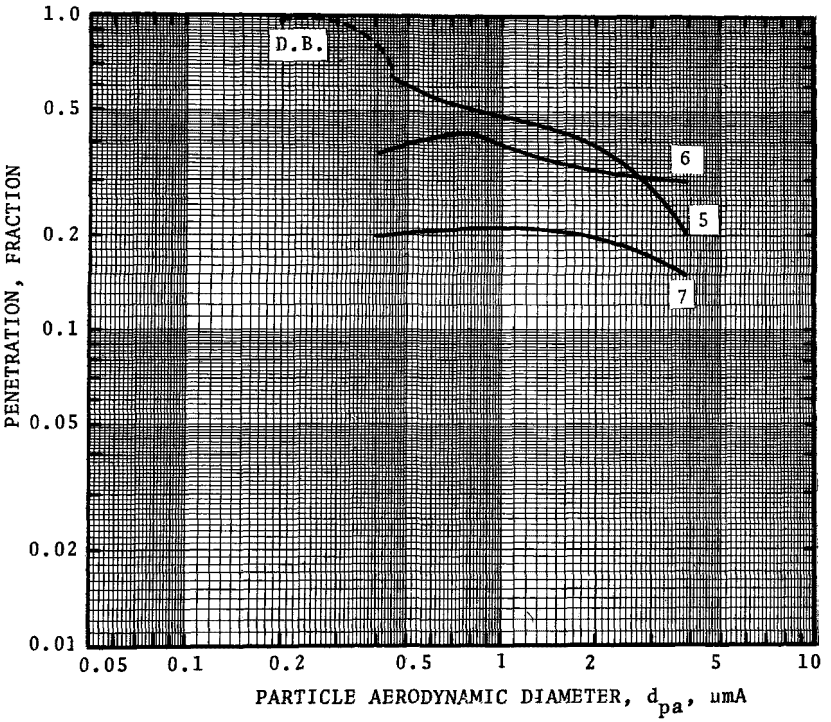

Figure 14. Particle penetration for cascade impactor runs 5, 6 and 7 and diffusion battery runs 3-9 (inlet) and 10-12 (outlet).

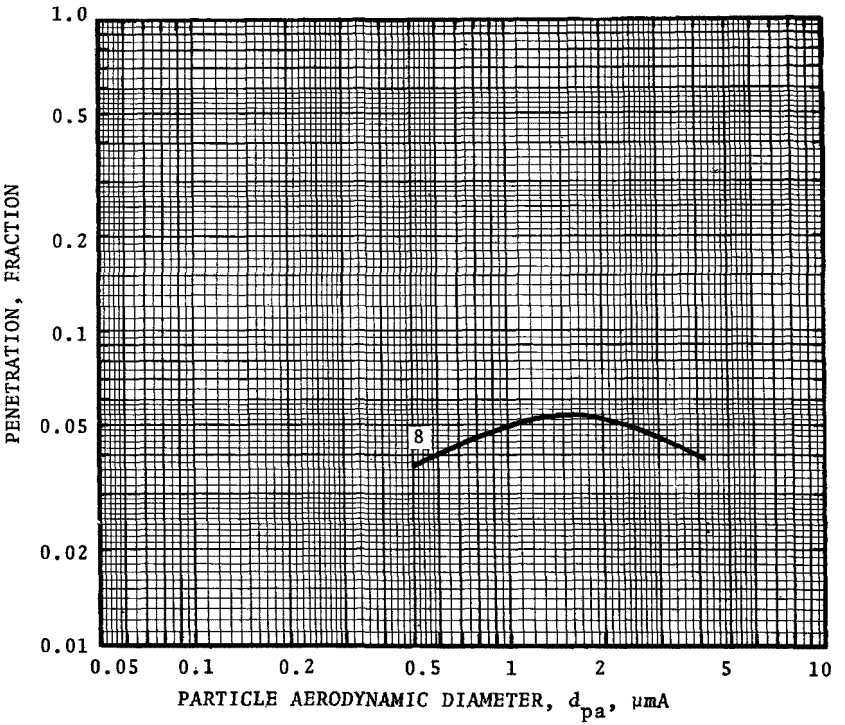

Figure 15. Particle penetration for cascade impactor run 8.

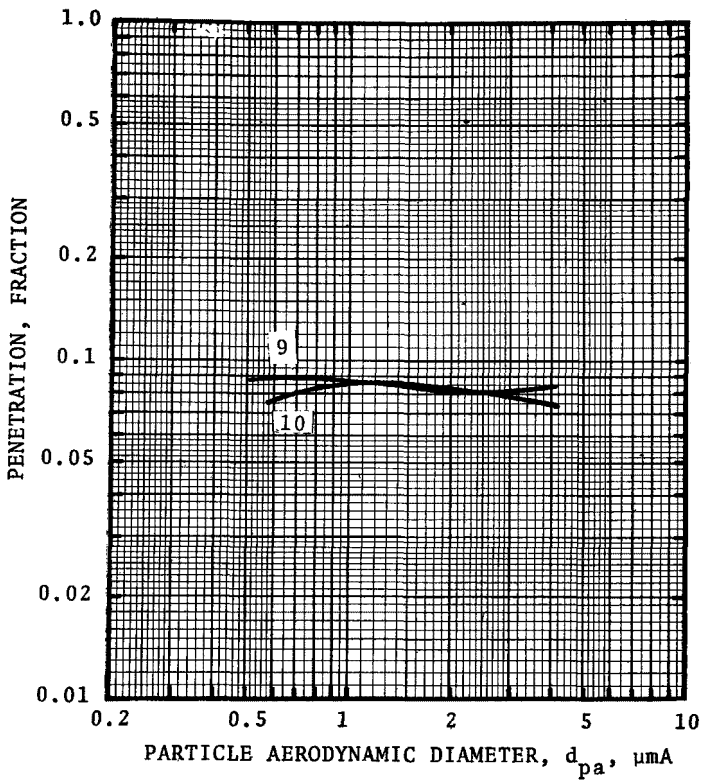

Figure 16. Particle penetration for cascade impactor runs 9 and 10.

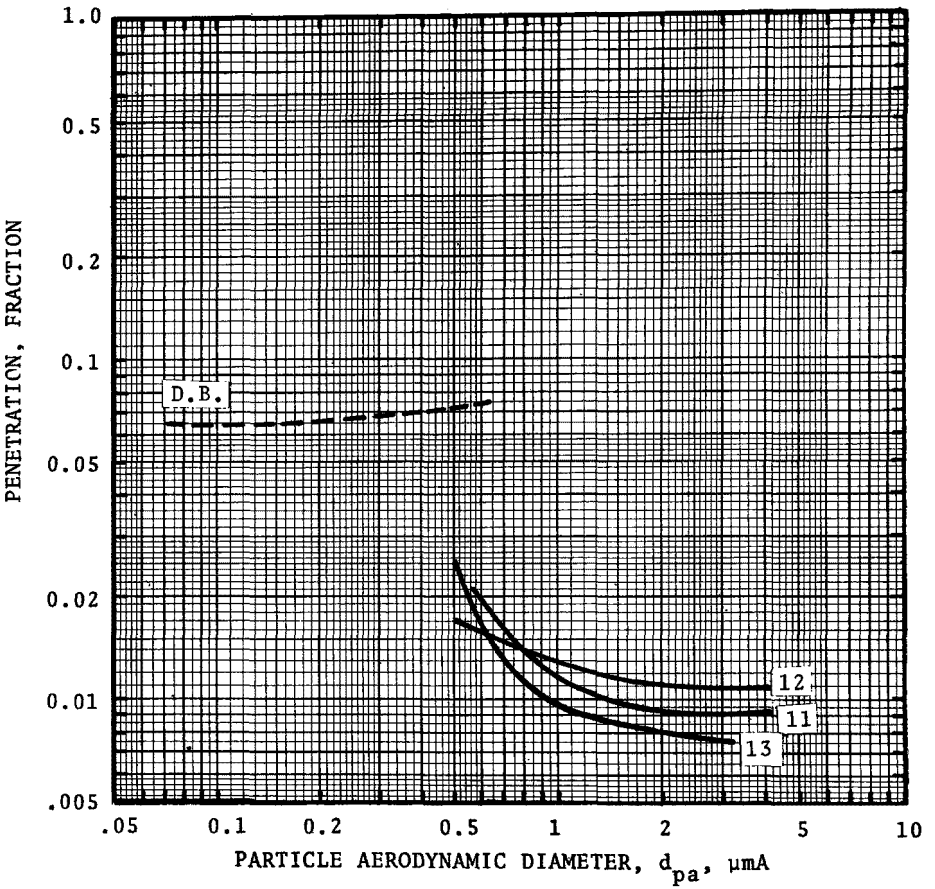

Figure 17. Particle penetration for cascade impactor runs 11, 12 and 13, and diffusion battery runs 15 and 16 (inlet) and 13 and 14 (outlet).

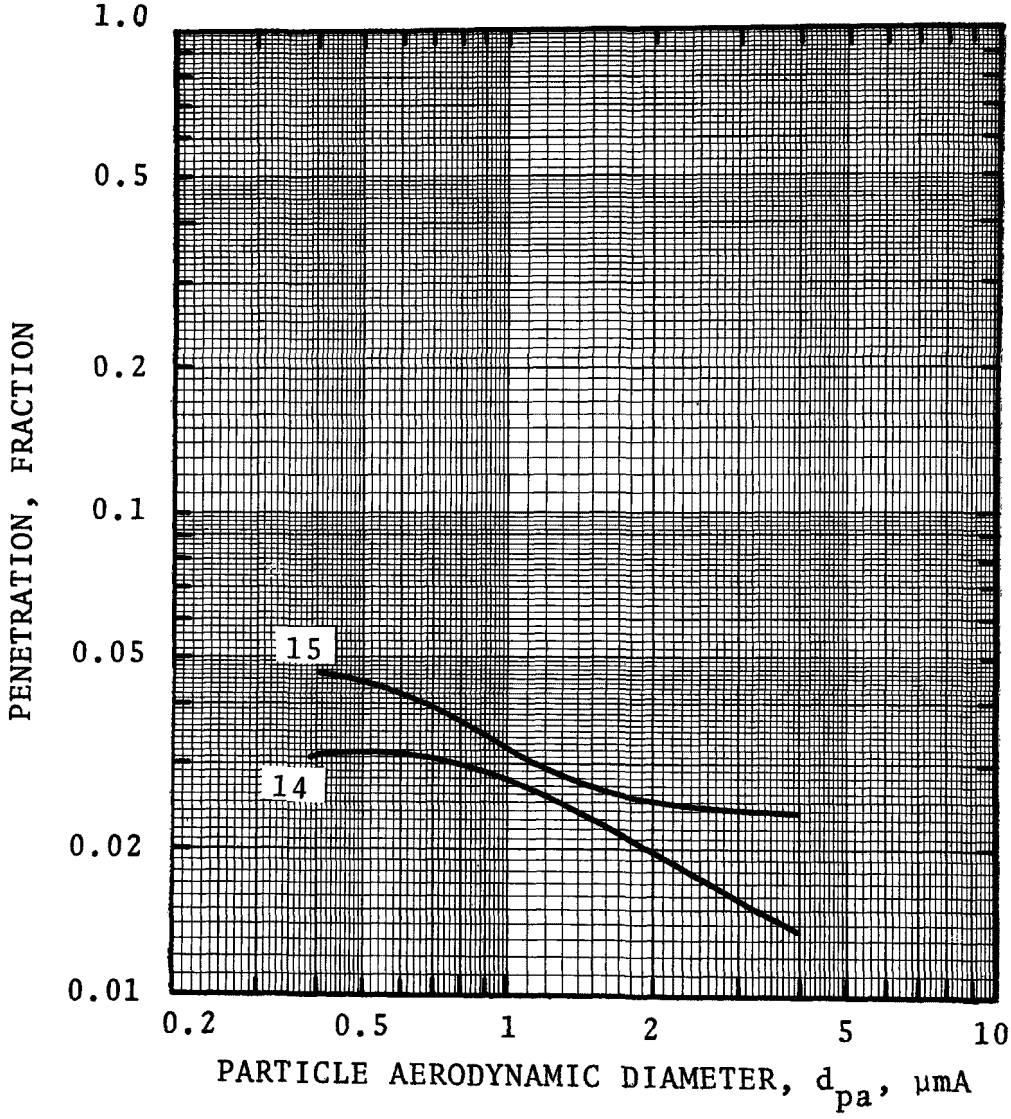

Figure 18. Particle penetration for cascade impactor runs 14 and 15.

OPERATING PROBLEMS

The primary operating problem with the system at first was the limiting capacity of the fan. Great amounts of excess air were getting into the system through all of the leaks, resulting in the fan running at its maximum capacity. For this reason the system could not pull enough gas through the scrubber and a large portion left through the top of the cupola. The amount of water that could be added to the system was also limited, which in turn affected the scrubber efficiency.

Once most of these leaks were patched, however, the fan amperage dropped well below the limit, and the system could be adjusted easily.

The scrubber liquor was another operational problem. Since the cyclone entrainment separator was not working effectively, much of the water which captured the particles was carried over, through the fan and out the stack. The scrubber liquor was recycled and changed only at the end of each day which meant that the solids concentration increased as the day progressed. Reentrainment of this water, therefore, would mean higher outlet loadings since this extra weight was considered in the emission rates.

Corrosion had a severe effect on the system operation because it was the cause of the excessive leakage of air into the scrubber and entrainment separator.

Another problem with the system was the absence of a cap on the cupola top. This allowed the gases to escape through the top. Some of the gases do not pass through the scrubber and therefore are not treated effectively, which in turn caused a visible emission problem. This was alleviated by capping the cupola top subsequent to our tests.

ECONOMICS

The scrubber system was built about ten years ago with substantial participation by the foundry. Consequently, the cost

was distributed among several purchased components, contracted work, and foundry-performed work. Records of the costs were not kept in one place and it was not possible to obtain precise data on the sub-system costs.

The operating cost for the blower (300 kW motor) was about $72.00 per day, based on eight hours use per day.

SECTION 6

PERFORMANCE COMPARISON

INTRODUCTION

All three scrubbers evaluated fall within the general classification of gas atomized spray scrubbers. The AAF venturi is most like a conventional venturi scrubber. The performance of gas atomized scrubbers depends on many factors which involve both the properties of the dust to be collected and the operating conditions of the scrubber. Yung, et al. (1977a) have modeled the performance of venturis assuming collection results from particle impaction on the liquid drops atomized in the venturi throat. The important parameters are particle aerodynamic impaction diameter, liquid drop diameter, amount of liquid, and relative velocity between the particles and the liquid. The energy used by a venturi goes primarily into achievement of high relative velocities and is manifested in the pressure loss.

PRESSURE LOSS

Yung, et al. (1977b) have derived a relatively simple model for the pressure loss in a venturi:

$$\Delta P = 1 \times 10^{-3} \; u_{de}^{*} \; u_{Gt}^{2} \left(\frac{Q_L}{Q_G} \right) \qquad (1)$$

where: ΔP = pressure drop, cm W.C.

u_{de}^{*} = ratio of the velocity attained by the liquid drops at the throat exit to the gas velocity, dimensionless

u_{Gt} = gas velocity in throat, cm/s

Q_L = liquid volume flow rate, cm^3/s

Q_G = gas volume flow rate, cm^3/s

This model is applicable to large venturis in which the predominant energy loss mechanism is the acceleration of the liquid drops. The term "u^*_{de}" is not ususally measured and can be considered an empirical constant. It has a direct mathematical relation to the venturi throat length under certain conditions, however. If the drop acceleration takes place in a constant area section and the initial drop velocity is insignificant then,

$$u^*_{de} = 2[1 - x^2 + (x^4 - x^2)^{0.5}] \qquad (2)$$

where: $$x = 1 + \frac{3\ell_t \, C_{Do} \, \rho_G}{16 \, d_d \, \rho_L} \qquad (3)$$

ℓ_t = venturi throat length, cm
C_{Do} = drop drag coefficient at throat inlet, dimensionless
ρ_G = gas density, g/cm^3
d_d = drop diameter, cm
ρ_L = liquid density, g/cm^3

For simplicity the drop diameter is taken as the Sauter mean diameter resulting from gas atomization as predicted by the Nukiyama-Tanasawa relation.

PARTICLE COLLECTION

Yung, et al. (1977a) found that the assumption that particle collection occurs primarily in the constant area throat section is often valid and greatly simplifies the performance prediction. In the throat section the particle penetration reduces to:

$$\frac{\ln Pt(d_p)}{B} = \frac{1}{K_{po}(1-u^*_{de}) + 0.7}\left[4\,K_{po}\,(1-u^*_{de})^{1.5} + 4.2\,(1-u^*_{de})^{0.5}\right.$$

$$\left. - 5.02\,K_{po}^{0.5}\left(1-u^*_{de} + \frac{0.7}{K_{po}}\right)\tan^{-1}\left(\frac{(1-u^*_{de})\,K_{po}}{0.7}\right)^{0.5}\right]$$

$$- \frac{1}{K_{po} + 0.7}\left[4\,K_{po} + 4.2 - 5.02\,K_{po}^{0.5}\left(1 + \frac{0.7}{K_{po}}\right)\tan^{-1}\left(\frac{K_{po}}{0.7}\right)^{0.5}\right] \qquad (4)$$

where:
$$B = \left(\frac{Q_L}{Q_G}\right)\left(\frac{\rho_L}{\rho_G}\right)\left(\frac{1}{C_{Do}}\right) \qquad (5)$$

$$K_{po} = \frac{C'\,d_p^2\,\rho_p\,u_{Gt}}{9\,\mu_G\,d_d} = \text{inertial parameter based on throat velocity, dimensionless} \qquad (6)$$

and, C' = Cunningham slip factor, dimensionless
d_p = particle diameter, cm
ρ_p = particle density, g/cm^3
μ_G = gas viscosity, poise

Equation (4) sometimes slightly underestimates the particle collection occurring in a venturi scrubber. For most industrial venturi scrubbers, particle collection can be predicted closely by neglecting the first term in the right hand side of equation (4).

The overall penetration prediction requires the integration of equation (4) over the inlet dust particle size distribution.

VARIABLE ROD MODULE VENTURI SCRUBBER COMPARISON

The variable rod module venturi is essentially several rectangular jets in parallel.

Pressure Drop

The exact geometry of the venturi rod module was not made available. Thus, throat length and throat gas velocity were not known, and the measured pressure drop could not be compared to that predicted by equation (1).

Particle Collection

Since "u^*_{de}" was not known from the geometry, penetration predictions for a range of values were made and are shown in Figures 19 and 20. The conditions used are shown in Table 19. The closest fit to the data occurred for u^*_{de} = 0.75 which corresponds to a throat length of 27 cm and a throat gas velocity of 11,700 cm/s, using equations (1) to (3).

TABLE 19. CONDITIONS FOR VARIABLE ROD VENTURI PERFORMANCE PREDICTIONS

ΔP =	178 cm W.C.			
Q_L/Q_G =	0.00168			
ρ_L =	1 g/cm^3			
ρ_G =	0.9 kg/m^3			
μ_G =	1.89 x 10^{-4} g/cm-s			
u^*_{de} =	1.0	0.75	0.5	
u_{Gt} =	10,140	11,710	14,340	cm/s
d_d =	107	101	93	µm
C_{Do} =	0.56	0.55	0.53	
B =	3.32	3.42	3.52	
ℓ_t =	∞	27	6.3	cm

Based on an approximate angle of free jet divergence of 20° and a spacing between rods equal to the rod radius, it was estimated that the rod diameter was 7.2 cm (2.8 in.), which was within reason.

The overall penetration was calculated on averaged cascade impactor data. For gray iron operation (d_{pg} = 0.91 µmA, σ_g = 1.6)

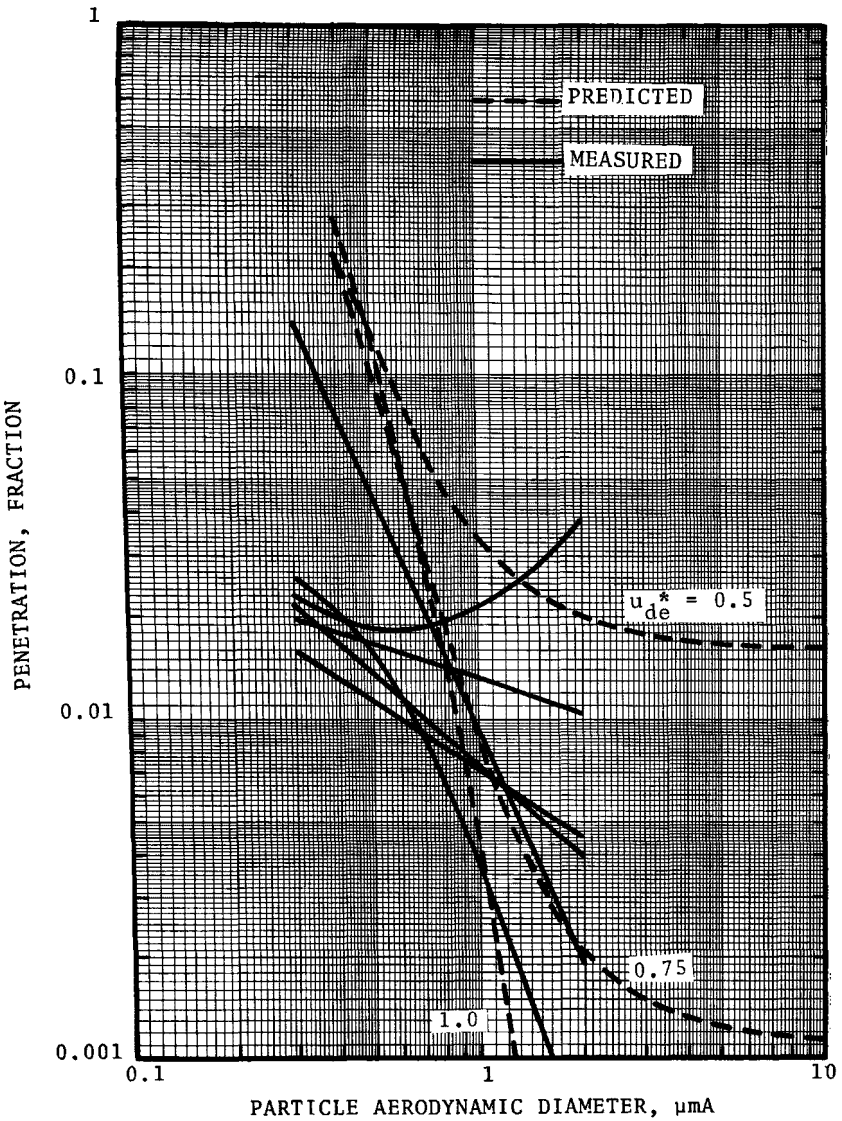

Figure 19. Comparison of predicted and measured penetrations for the NDC venturi during gray iron operation.

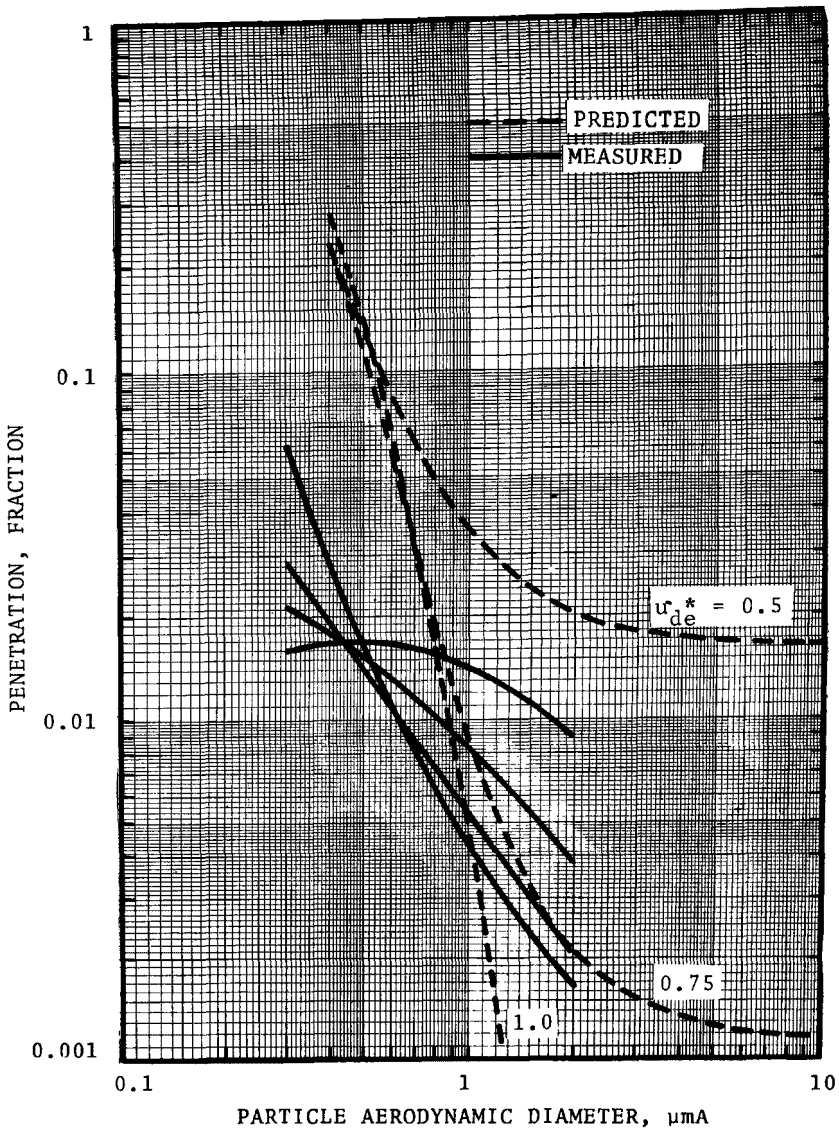

Figure 20. Comparison of predicted and measured penetration for the NDC venturi during ductile iron operation

a penetration of 4.1% was predicted and for ductile iron operation (d_{pg} = 0.57 μmA, σ_g = 1.7) a penetration of 16.2% was predicted. The data indicated the overall penetration was between 1% and 2.5%, which meant that the size distribution used in the predictions was not correct for sizes larger than about 3 μmA.

Discussion

The model assumes that collection is by inertial impaction on drops, occurring only in the throat region of the venturi. The data agree with the model in the range of 0.8 to 2.0 μmA diameters but show greater efficiency below 0.8 μmA. Thus, the model is fairly close for the larger particles of interest. However, as particle diameter decreases below 1 μmA diameter, forces other than inertia, such as flux forces and Brownian motion, become important.

Diffusiophoresis, and thermophoresis, two of the flux force/condensation (F/C) mechanisms are effective in regions where the liquid spray drops are cooler than the gas and the gas is saturated. Some condensation may have caused particle growth between the inlet sampling port and the variable rod module. Here the prescrubber sprays may have been a few degrees cooler than the gas, so that enough particle growth could have occurred prior to the venturi rod module to increase the collection efficiency of the smaller particles.

F/C effects could have caused the cooling spray drops to collect fine particles in the cooling section of the tower. The cooling spray water temperature was about 20°C lower than the gas temperature. Collection by Brownian diffusion would not be important in the size regime that was measured in these tests.

Another section of the system where small particle collection could have occurred was the section containing the two blowers in series. The high velocity and extreme turbulence in the blowers may have been effective in causing particle collection.

AAF KINPACTOR VENTURI SCRUBBER COMPARISON

The American Air Filter venturi is a classical venturi with a rectangular throat. The throat width is automatically controlled

to maintain a pressure drop of about 110 cm W.C.

Pressure Drop

Since the throat width was automatically controlled the throat area and gas velocity were not known with any precision. The maximum throat area possible was 0.361 m^2. The throat length was not known either. Thus, direct comparison of pressure drop measured with equation (1) was not possible.

Particle Collection

In many venturis the ratio of drop velocity to gas velocity at the throat exit (u^*_{de}) is about 0.8, and this value will be used in the prediction. The liquid to gas ratio used is based on the gas flow rate at the outlet for runs 12 and 13 (20 Am^3/s) and 80% of the stated liquid flow rate (33 ℓ/s). Table 20 presents the conditions used for the performance prediction.

TABLE 20. CONDITIONS FOR AAF VENTURI PERFORMANCE PREDICTION

ΔP	= 110 cm W.C.
Q_L/Q_G	= 0.0017
ρ_L	= 1.0 g/cm^3
ρ_G	= 0.79 kg/m^3
μ_G	= 1.6 x 10^{-4} g/cm-s
u^*_{de}	= 0.8
u_{Gt}	= 8,860 cm/s
d_d	= 104 μm
C_{Do}	= 0.58
B	= 3.37
ℓ_t	= 41 cm

The comparison of prediction with the data is shown in Figure 21. The measured penetration is also shown corrected for

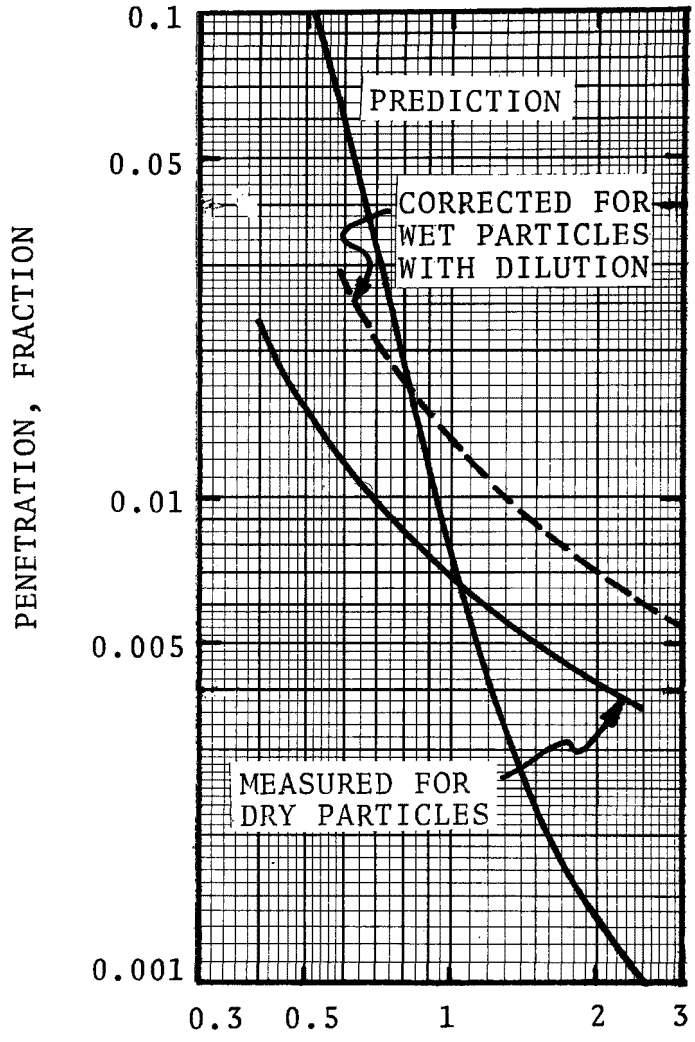

Figure 21. Comparison of predicted and measured penetration for the average of runs 12 and 13 of the AAF venturi

dilution and for a diameter increase to account for the fact that the measurements were made with heated impactors. Based on an average d_{pg} = 1 μmA and σ_g = 3 for the inlet dust the overall penetration was predicted to be about 15% while the measured penetration was about 3%.

Discussion

In order to compare the model with experiment a few important factors need to be noted:

1. Heated impactors - As explained previously the inlet and outlet size distributions were determined using heated cascade impactors. Based on previous experience it was expected that the mass median diameters of the actual wet borax particle size distributions were up to 1.5 times the sizes measured in the heated impactors. The high solubility of borax was the primary reason for the difference. Thus the venturi was collecting larger particles than those measured in the heated impactor. In order to compare the experimental results with the prediction it is necessary to plot experimental penetration against the actual (wet) particle size rather than the dried particle size. This correction causes the measured penetration curve in Figure 21 to shift toward larger particle diameters because Figure 10 is on the dry particle size basis.

2. System leaks - The actual scrubber penetrations could also be different from those based on the impactor data because of dilution of the outlet by air leaks into the system, which probably did occur. Dilution of the outlet stream would cause the actual penetrations to be greater than those measured by a factor equal to the dilution factor. The outlet concentration may have been diluted as much as 25%. The dashed line on Figure 21 includes the effects of 25% dilution and 1.5 times particle growth on measured data.

3. Collection mechanisms - The model for venturi performance assumes particle collection by inertial impaction on drops in the throat region of the venturi. This model does not account

for forces other than inertia which can effect submicron particle collection. Thus, in the region below about 0.5 μmA the predicted penetration and the experimental penetration are expected to differ.

Another important phenomenon is the collection of particles of all sizes due to solution-induced condensation. Borax ($Na_2B_4O_7$) is highly soluble in water. If the scrubber liquor became more concentrated than would be in equilibrium with the vapor, it is conceivable that particles could be swept toward the liquid as water vapor moves to condense on it. The liquid drops which contain dissolved borax have a reduced vapor pressure which induces the condensation which causes the growth in particle size manifested in the differences between wet and dry particle sizes.

Some of this dissolution and condensation will have occurred in the quench section upstream of the venturi. However, because of the large amount of liquid injected at the venturi these mechanisms may still be causing particle collection and growth downstream of the venturi. Growth or collection of the submicron particles after the inlet sampling point, either before or after the venturi would explain some of the differences between the predicted and the experimental penetrations.

Condensation can also occur when the vapor pressure of the water is reduced because it is at a lower temperature than the adiabatic saturation temperature of the gas. This cause of condensation was not significant here because there was very little cooling of the scrubber liquor.

4. Sensitivity of prediction to L/G ratio - The predicted curve is very sensitive to the liquid to gas volume flow rate ratio (L/G) for particle diameters above 1.0 μmA. A 25% decrease in the L/G ratio would cause the prediction to agree closely with the data. Since neither the inlet gas flow rate nor the liquid flow rate are known precisely, it is possible that the actual L/G ratio was lower than the value used in the prediction.

5. Entrainment - The carry-over from the cyclone was so heavy that precutters had to be used on the outlet sampling probe. It

was possible that some smaller entrainment drops, containing dissolved borax, penetrated the precutters or were shattered in the precutters and were collected in the heated impactors. Since the venturi model assumed that no entrainment carry-over occurred, the actual penetrations would be greater than the model predictions as seen in Figure 21.

These five factors help explain the differences between the model prediction and the data. The many factors and uncertainties involved are enough to preclude any judgment of the accuracy of the model.

GAS-ATOMIZED SPRAY SCRUBBER COMPARISONS

The gas-atomized spray scrubber had a throat section that was a rectangular orifice, whose width could be varied to adjust the pressure drop.

Pressure Drop

The geometry of this scrubber was well known except for the "throat length." Since the throat was an orifice the physical length was only a fraction of a centimeter. However, a free jet will not expand immediately but will continue straight for a few centimeters. A straight section length of 10 cm was chosen and as seen from Table 21 a reasonable pressure drop was predicted for some of the run sets. Predicted pressure drop for two of the run sets was very poor indicating either an error in measurement or the assumed straight section throat length was too large.

Particle Collection

The scrubber parameters are known or estimated from the average of the conditions for the sets of runs and shown in Tables 21 and 22. The predicted particle penetrations are shown compared to the average of the run sets in Figures 22-26. The solid (measurement) curves represent the measured penetration without accounting for leakage. The dashed curves assume that the outlet was diluted by the factor listed in Table 22 which is based on the data in Table 14.

The overall penetration predictions for the average log-normal inlet dust distribution based on the cascade impactor data are shown in Table 23.

TABLE 21. PRESSURE DROP COMPARISON FOR THE GAS ATOMIZED SPRAY SCRUBBER

Run Set	u_{Gt} cm/s	Q_L/Q_G	u^*_{de}	Measured ΔP cm W.C.	Predicted ΔP cm W.C.
5,6,7	10,600	0.0011	0.61	79	78
8	23,200	0.0009	0.70	83	349
9,10	24,400	0.0008	0.70	82	342
11,12,13	10,400	0.0031	0.43	103	148
14,15	10,400	0.0014	0.58	88	91

Note: Assumed ℓ_t = 10 cm

TABLE 22. CONDITIONS FOR GAS-ATOMIZED SPRAY SCRUBBER PERFORMANCE PREDICTION

Run Set	ρ_L g/cm³	ρ_G kg/m³	μ_G g/cm-s	d_d μm	C_{Do}	B	Dil[1]
5,6,7	1.0	0.72	2.1×10^{-4}	79	0.68	2.26	1.23
8	1.0	0.70	2.2×10^{-4}	45	0.64	2.00	1.27
9,10	1.0	0.36	4.1×10^{-4}	40	1.10	2.02	1.88
11,12,13	1.0	0.93	1.7×10^{-4}	200	0.46	7.30	1.79
14,15	1.0	0.80	2.0×10^{-4}	94	0.61	2.86	1.22

[1]Dil is the ratio of measured outlet to inlet volume flow rates at standard conditions.

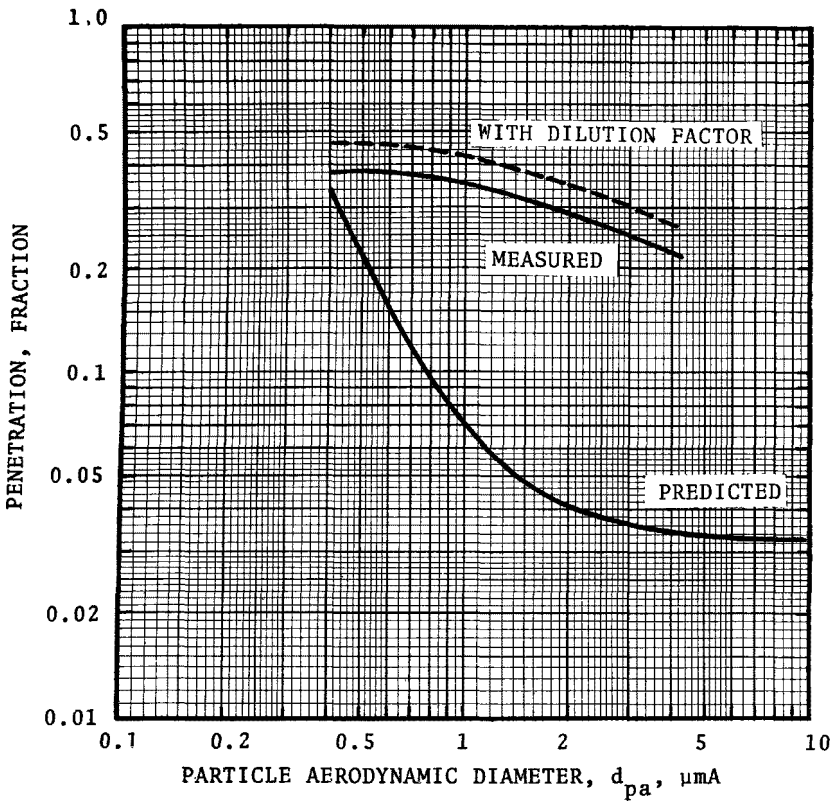

Figure 22. Comparison of predicted with measured penetration for average of runs 5, 6 and 7, for the gas-atomized scrubber.

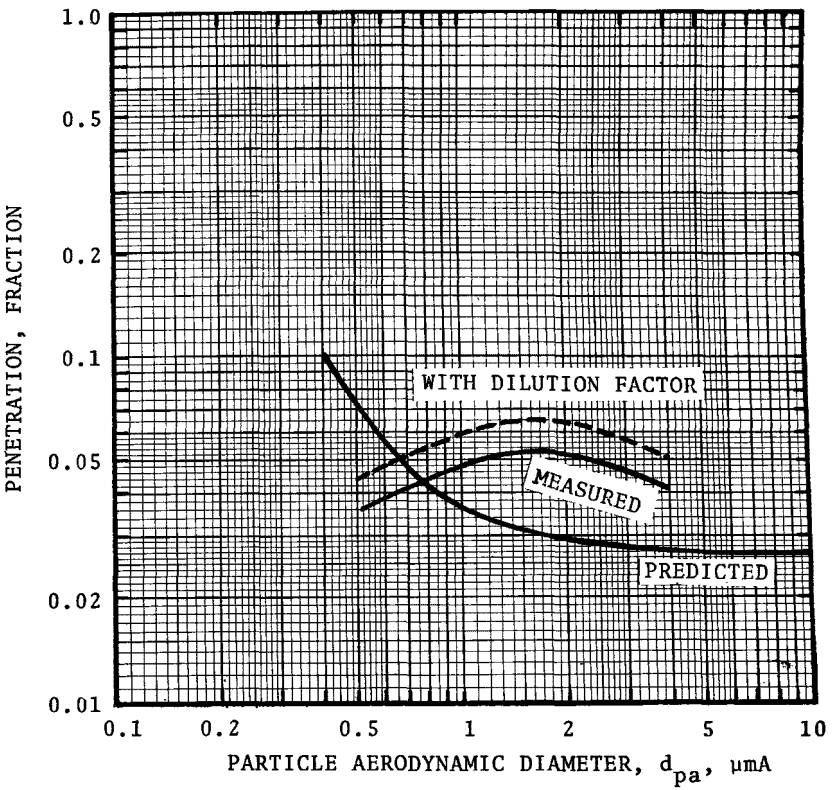

Figure 23. Comparison of predicted with measured penetration for run 8 for the gas-atomized scrubber.

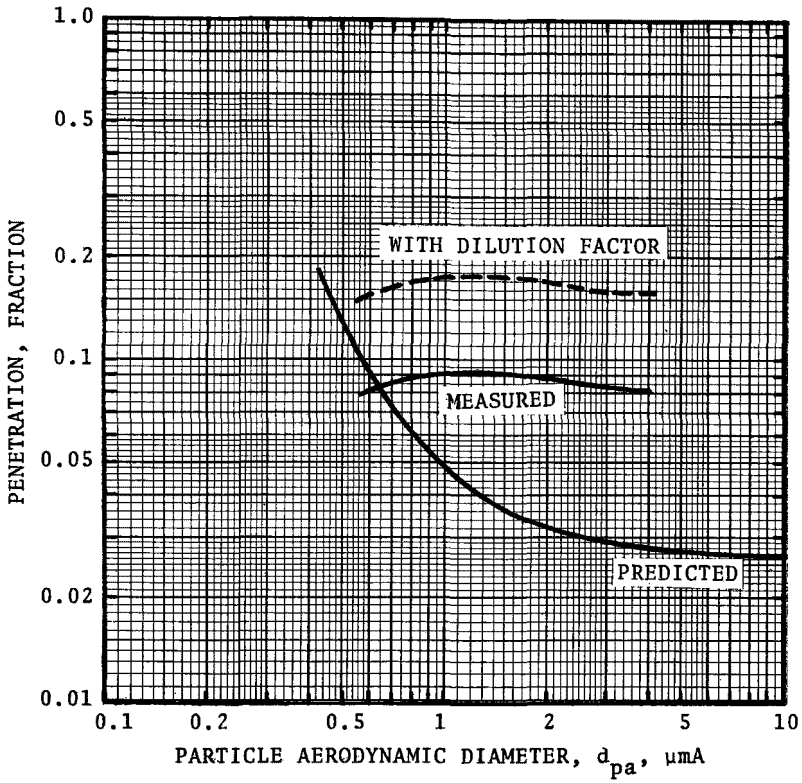

Figure 24. Comparison of predicted with measured penetration for average of runs 9 and 10 for the gas-atomized scrubber.

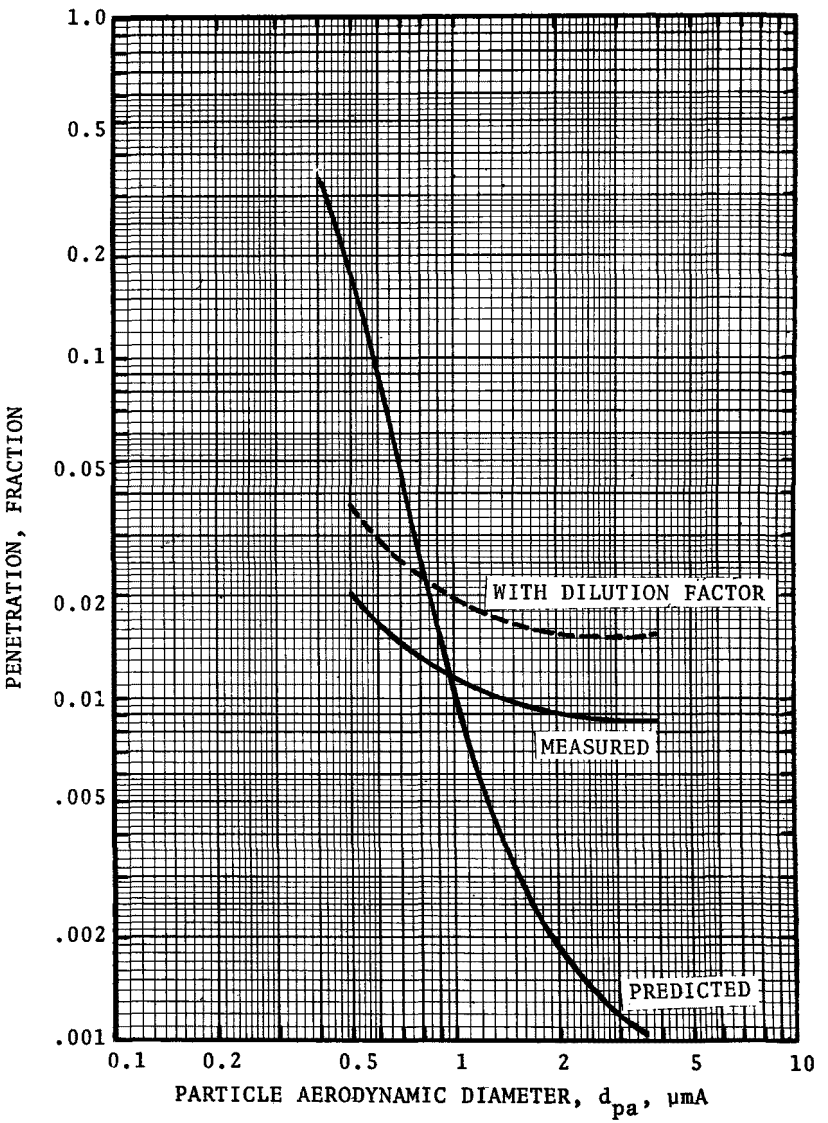

Figure 25. Comparison of predicted with measured penetration for average of runs 11, 12 and 13 for the gas-atomized scrubber.

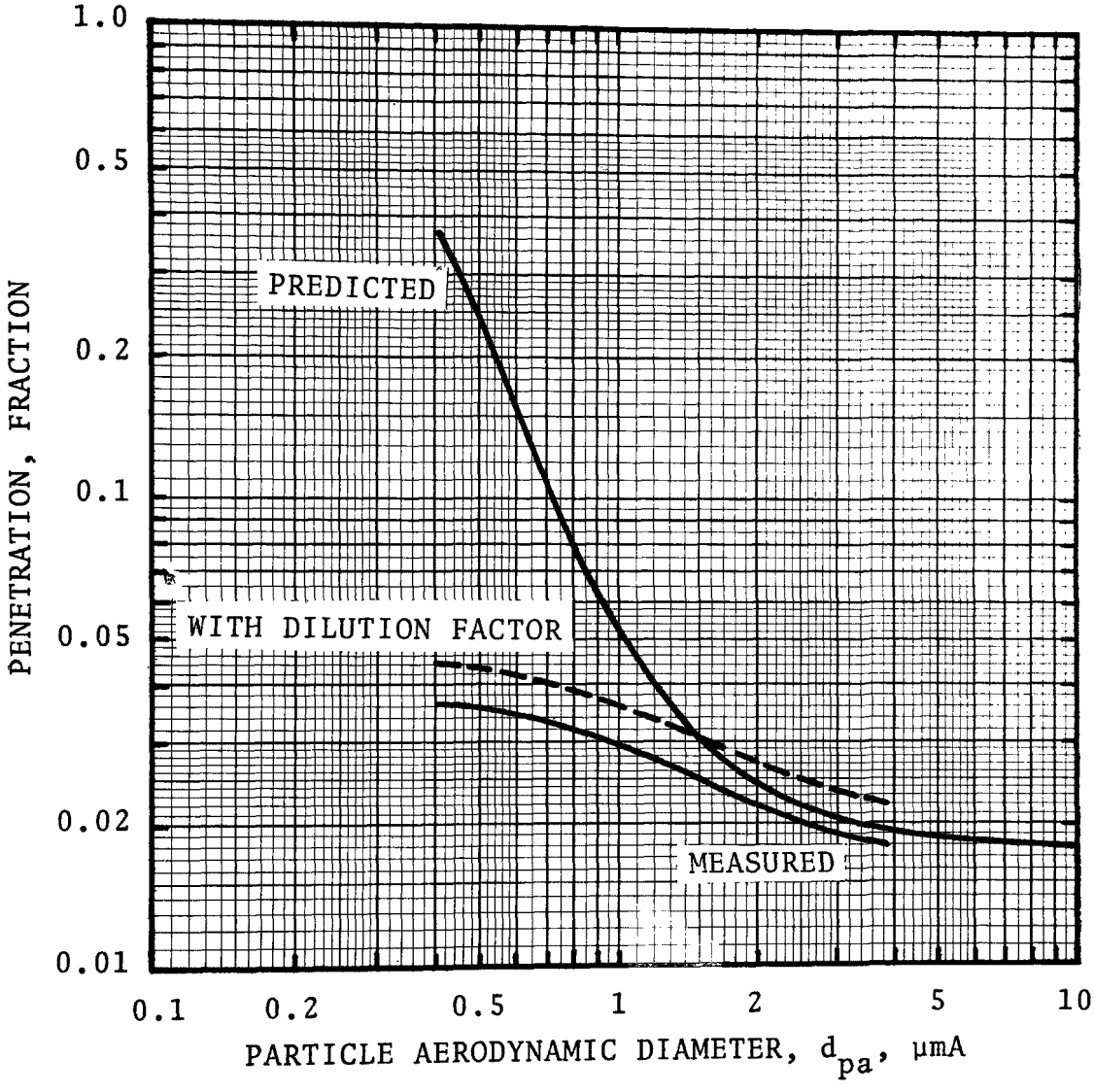

Figure 26. Comparison of predicted with measured penetration for average of runs 14 and 15 for the gas-atomized scrubber.

TABLE 23. OVERALL PENETRATION COMPARISON FOR THE GAS-ATOMIZED SPRAY SCRUBBER

Run Set	Measured * $\overline{Pt}$, %	Predicted $\overline{Pt}$, %
5,6,7	13	47
8	5	26
9,10	5	33
11,12,13	7	44
14,15	15	45

Note: Assumed d_{pg} = 0.4 μmA, σ_g = 2.5

* Neglecting outlet precutter dry weight gain.

Discussion

The comparison of predicted and measured penetration leads to the following observations:

1. The predictions are generally close to the experimental results for particles around 1 μmA diameter. Runs 5, 6, and 7 have the poorest fit. Although the operating conditions for these runs were similar to those of runs 14 and 15, the experimental penetration was greater. This may be due to the fact that the gas flow rate was higher in runs 5, 6, and 7 which could mean more leakage and could cause more entrainment carryover at the outlet. The effect of L/G ratio on the model predictions is shown by comparing the predicted penetrations of these two run sets. The main difference in the operating conditions was that runs 14 and 15 had a 45% higher L/G ratio than runs 5, 6 and 7.

2. Predicted penetration for sub-micron particles is generally higher than measured. This may be due to condensation caused by the cool duct walls and the cool scrubber liquid which had low temperatures due to the cold ambient air (0°C). Leaks of the cold ambient air into the system would also have caused condensation.

3. Predicted penetration is generally lower than measured for particles larger than about 1 μmA diameter. There are several plausible causes of this disparity:

a. Entrainment not collected in the entrainment separator would yield particles in the larger size range. The cyclone separator was known to be inefficient although its performance was improved by internal modifications and leak patching. This inefficiency was clearly demonstrated by noticeable liquid drops at the outlet stack where the sampling crew was working, and by the precutter mass collections.

b. Imprecise knowledge of the liquid flow rate can cause the prediction to be substantially incorrect in the larger particle size range. This effect becomes more serious as the liquid/gas ratio decreases, as seen by comparing the prediction of runs 4, 5, and 7 with that of runs 14 and 15.

4. Predicted overall penetration was generally higher than measured. This difference is probably due primarily to the assumption that the size distribution is log-normal with the same standard deviation for all particles less than 0.4 μmA (d_{pg}). Condensation probably affected the log-normality of the small size distribution. Also, the penetration model over-predicted the penetration of the smaller particles which would definitely cause the overall penetration prediction to be too high.

In conclusion, with all the real effects considered, the model provides an adequate prediction. Predictions for several of the runs, notably 8, 11, 12, 13, 14, and 15, were quite good.

SECTION 7

PERFORMANCE TEST METHOD

The approach used in these scrubber evaluations involved obtaining experimental collection efficiency data, acquiring information on system characteristics and behavior, and performing computations which made use of the performance data and mathematical models. Over the course of the program the methods and apparatus used generally were improved and modified to suit each specific test situation; however the main features remained similar and are described here.

The most important experimental measurements were those regarding particle size and concentration. Cascade impactors were used to determine particle diameters larger than 0.3 μmA. The Air Pollution Technology, Inc. portable screen diffusion battery (A.P.T. - S.D.B.) was used for particle size determination in the diameter range from 0.01 μm to 0.1 μm (actual). The apparatus and methods used are outlined below:

1. Gas velocity distribution and parameters were measured at the inlet and outlet of the scrubber in order to define the following:

    a. Conditions required for isokinetic sampling.

    b. Particle mass concentration per unit volume of dry gas, which is needed to provide a consistent basis for comparing inlet with outlet size distributions in the computation of efficiency.

    c. Gas flow rate.

    d. Amount of liquid entrainment in the scrubber outlet.

Methods to measure these parameters are tabulated in the table on the following page.

TABLE 24. MEASURING EQUIPMENT AND METHODS

Parameter	Equipment	Method
Gas velocity and flow rate	Standard pitot tube or calibrated type "S" pitot tube; differential pressure gauge.	EPA Method 1; EPA Method 2.
Gas temperature	Calibrated thermocouple or mercury filled glass-bulb thermometer.	
Humidity	Wet bulb - dry bulb thermometers.	Wet and dry bulb temperature measurement on a flowing sample withdrawn from the duct.
Pressure	Inclined water manometer or a pressure gauge.	Measured by means of a static pressure tube inserted in the duct.

2. The most essential part of a scrubber performance test is the determination of particle size distribution and concentration (loading) in the inlet and outlet of the scrubber. For accurate determination of particle size distribution, a collection mechanism that collects particles and causes neither formation nor breakup of aggregates is necessary. Cascade impactors come close to meeting these requirements.

In a cascade impactor particles are classified by inertial impaction according to their mass. The larger ones are collected on the plate opposite the first stage and the smallest on the plate opposite the last stage. A.P.T. used the University of Washington Mark III source test cascade impactor for particle size fractionation. This impactor classifies particles into seven size ranges and is capable of sizing particles down to about 0.1 μm diameter (actual). All impactors were calibrated in the laboratory according to EPA guidelines, see Calvert, et al. (1976) and Harris (1977) on calibration method.

In order to minimize probe losses, tests were made with the impactors in the duct and with the inlet nozzles appro-

priately sized to give isokinetic sampling. A modified EPA Method 5 sampling train was used to monitor the sample gas flow rate. Figure 27 shows the sampling train arrangement.

In some tests, a precutter was used to remove either the large particles from inlet samples or the entrained liquid from outlet samples. A round jet impactor was found to work satisfactorily as the precutter and was adopted for use for both inlet and outlet sampling. The impactors were either given time to reach the duct gas temperature or heated to prevent condensation.

To increase the weighing accuracy, lightweight substrates were used on the collection plates. Generally, either greased aluminum foil or a glass fiber filter paper substrate was used. Impactor substrates and backup filters were weighed to the nearest tenth milligram (10^{-4}g) by using an analytical balance.

Particle size distribution and loading measurements were conducted simultaneously at the scrubber inlet and outlet. This minimizes the effects of particle size distribution changes which may result from fluctuations in the operation parameters. The sampler was held at one location in the duct for the duration of each sampling run. This is an adequate technique for obtaining good samples of particles smaller than a few microns in diameter because they are generally well distributed across the duct.

Blank impactor runs were performed periodically to assure that the greased aluminum substrates did not react with the stack gases or lose weight. A blank impactor run consists of an impactor preceded by two glass fiber filters and run at identical sample conditions as the actual smapling runs.

3. In-stack filter samples were taken to obtain total particulate loadings and overall collection efficiencies of the system. The sampling train arrangement was the same as the cascade impactor train (Figure 27) with the cascade impactor replaced by a filter.

4. Inertial impaction devices such as cascade impactors are normally insufficient for sizing particles smaller than 0.1 to

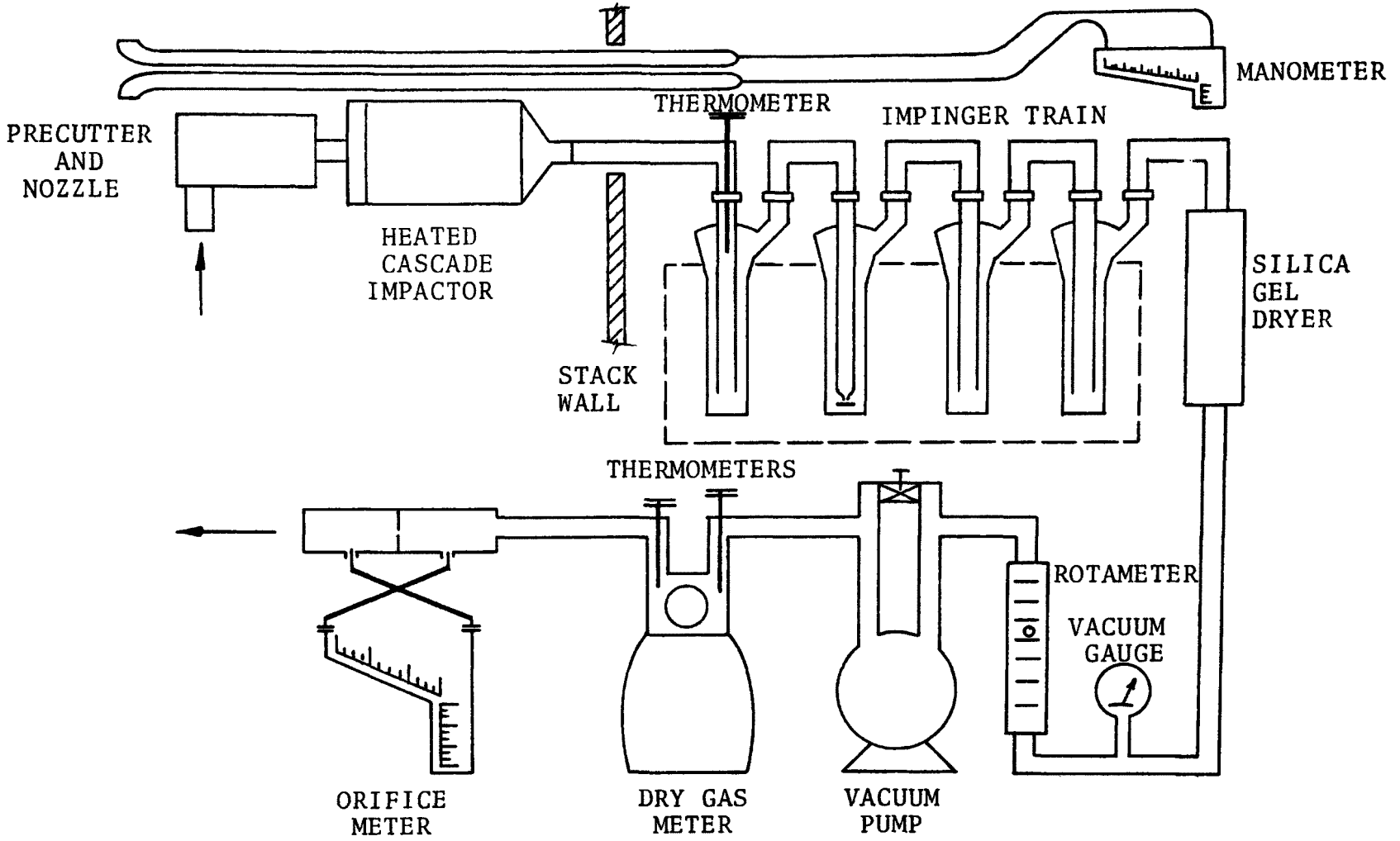

Figure 27 - Modified EPA sampling train with in-stack cascade impactor

0.3 μm (actual diameter). Size fractionation of these particles may be accomplished by diffusional collection devices (diffusion batteries) which may consist of closely spaced parallel plates, long, thin tubes, or an array of wire screens. Parallel plate and tube diffusion batteries require many pumps, dilution apparatus, and other bulky equipment which prove to be cumbersome in field use. For this and other reasons, Air Pollution Technology, Inc. developed and uses a portable screen diffusion battery which is lighter and more portable than previous devices.

The screen diffusion battery utilizes a series of layered screens intermittently separated for sampling purposes (Figure 28). Size fractionation by the diffusion battery is detected by measuring the overall particle number concentrations of the gas stream entering and leaving a known number of screens. A condensation nuclei counter (CNC) is used to determine number concentrations. Concentrated aerosol samples must be diluted until compatible with the CNC (~10^6 particles/cm^3). Screen penetration data are then analyzed to determine size distribution and cumulative mass loading of the particulates in the stream. Cascade impactor and diffusion battery analyses often can be combined to obtain an overall characterization of the particulate size distribution (and scrubber penetration).

Fine particle size measurements with the diffusion battery were not taken simultaneously at the inlet and outlet of the scrubber system. During an impactor run, several inlet and outlet measurements were taken alternately with the S.D.B. Since the system remained fairly constant during each run, alternate inlet and outlet S.D.B. measurements were considered to approximate simultaneous sampling.

Each S.D.B. run consisted of a continuous series of CNC readings. Normally, CNC counts were taken at each diffusion battery stage in order of increasing number of screens and then the process was repeated until three to four sets of readings

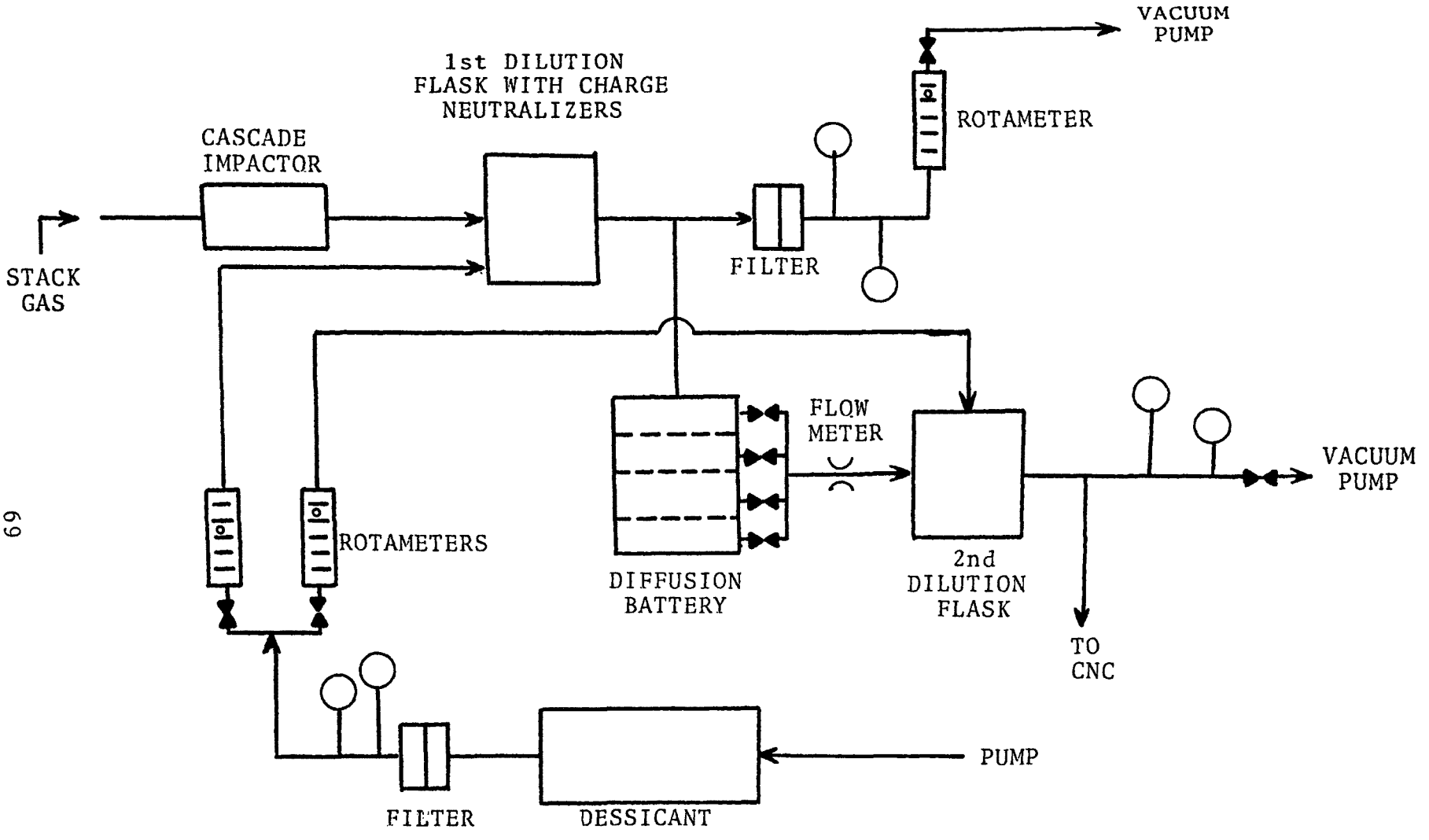

Figure 28. Schematic diagram of diffusion battery system.

were obtained. Continuous monitoring of flow, temperatures, and pressures enabled steady operation of the diffusion battery. Conditions in the duct (pressure, gas velocity, temperature, and water vapor content) were obtained during the impactor tests.

The size of particles entering the diffusion battery was limited by using a cascade impactor precutter on the instack end of the probe. Ioskinetic sampling was not maintained because the particles to be measured were too small to be segregated by inertial effects from bends in the gas stream. The sample stream entering the diffusion battery was immediately diluted with heated, dried, filtered air to control condensation. Two Polonium 210 charge neutralizers were inserted into the flask to eliminate electrostatic effects.

A portion of the resultant aerosol was directed through the diffusion battery and the outlet was diluted to a concentration measurable by the Gardner CNC. The aerosol from the second dilution flask was sampled with the Gardner CNC. The excess aerosol was exhausted through the vacuum pump. The excess aerosol from the first dilution was passed through an absolute filter and pumped to the atmosphere. The Gardner CNC was calibrated daily against a standard B.G.I. Pollack, Model P, CNC and found to read consistently 33% lower than the Pollack CNC for the concentration range used in these tests.

ERROR ANALYSIS

Sample Bias

It is important to note that the program objective is to investigate scrubber performance on fine particles and, consequently, it is not essential that the methods used be accurate for large particles. This makes the sampling simpler in the following ways:

1. Isokinetic conditions are not important for fine particles. For example, the error caused by sampling 4 μmA particles at a velocity 50% higher or lower than the gas stream velocity would only be about 2 or 3% of the concentration.

2. The fine particles will be well distributed in the gas stream, except in cases where streams with different particle concentrations have not had time to mix, so that generally single point sampling is sufficient. To illustrate, we may note that the Stokes stopping distance of a 3 μmA particle with an initial velocity of 15 m/s (50 ft/s) is about 0.04 cm (0.016") and for a 1 μmA diameter particle it is one ninth of that. Since the stopping distance is the maximum distance a particle can be displaced from a gas stream line by going around a right angle turn, it is obvious that fine particle distribution in the gas stream will be negligibly affected by flow direction changes.

3. The effect of a precutter on the size resolution of a cascade impactor is not significant in the size range of interest, so long as the precutter has a cut diameter larger than several microns.

Diffusion Battery

The screen diffusion battery was calibrated in the A.P.T. small particle laboratory. An aerosol of known size distribution was generated and passed through the diffusion battery. The total number concentration was measured with a condensation nuclei counter at the inlet and outlet of each S.D.B. stage. The penetration (percent) of particles was then calculated and plotted against solidity factors on semi-logarithmic paper. The experiment was repeated with the same aerosol until a smoothed average curve relating number penetration to solidity factor was obtained. From the smoothed curve, a correlation factor was found for computing the theoretical diffusion battery performance.

The scatter of data points about the smoothed (fitted) calibration curve represents the experimental error in the penetration measurement. This measurement error included meter reading error and the accuracy of the CNC. The measurement error was defined in terms of relative error, or the deviation from the averaged penetration value divided by the averaged value.

This procedure was repeated on other aerosols of known size distribution. The maximum relative error was then determined

from these experiments for each solidity factor. The maximum relative error for the screen diffusion battery determined by this method is 10.4% for solidity factors of 13, 26, and 40.

Cascade Impactors

Cascade impactors were used as the principal means of obtaining information about the inlet-outlet size distributions. It was important to understand the sources of error and how the error can be minimized.

The procedural errors include the accuracy of the weighing of the deposits, and reading of the test data such as temperature, gas volume, time, and pressures. The errors from the impactor design and construction include wall losses, accuracy and precision in construction of critical components, and particle reentrainment from the collection surface.

Some of the design and construction limitations can be reduced by procedures such as recovering the wall losses and by sampling at certain flow rates and times to reduce reentrainment errors and by calibration of the impactor. The experimental data obtained with commercial impactors were reported by Smith, et al. (1974). Smith, et al. (1974) reported that all impactors tested had appreciable wall losses for particle diameters above 10 microns. This error can be reduced by brushing the material from the wall onto appropriate collection disks. The flow velocity through the impactor jets should not be above 65 m/s to be absolutely certain of avoiding reentrainment of particles from the collection substrates. The extent of reentrainment will depend on the properties of the material and the amount of deposit. However, Rao (1975) reported that collection efficiency increased with increased particle load. When the particle weight is over 10 mg, part of the deposit may break away from the surface and migrate within the impactor. The lightweight deposit places importance on accurate weighing. The analysis of impactor errors was limited to the weighing error and in the calculation of collection efficiency error. The effects of weighing errors on the results of impactor tests have been analyzed by Sparks (1971).

An analysis of the weighing error using three different estimations was reported by Fegley, et al. (1975). The results indicate that, when the weight of sample per stage is less than 1 mg when weighed with a balance with a precision of 0.05 mg, the error in the fractional mass will be greater than 10%.

SECTION 8

DATA REDUCTION AND COMPUTATION METHOD

CASCADE IMPACTOR DATA ANALYSIS

In a cascade impactor particles are classified by inertial impaction according to their mass. The larger ones are collected on the plate opposite the first stage and the smallest on the plate opposite the last stage.

Once the stage "catches" have been measured, usually by weighing particle collection foils or papers, the data analysis is relatively simple. Generally the objective is to make a plot of particle diameter versus mass percent oversize or undersize and to represent the size distribution in terms of log-normal distribution parameters if possible. Thus, it is necessary to do the following:

1. Add all of the stage and filter collection weights to get the total particle mass collected.
2. Compute either:
   a. Cumulative percent collected as the gas flows through the succeeding stages. This is "percent oversize."
   b. Cumulative percent penetrating as the gas flows through succeeding stages. This is "percent undersize."
3. Compute the cut diameters for the impactor stages, taking into account gas viscosity (or temperature) and gas sampling flow rate. The equation is:

$$d_{pac} = K_{p50}^{0.5} \left(\frac{9\ \mu_G\ d_j}{u_j \times 10^{-8}} \right)^{0.5} \qquad (7)$$

where: d_{pac} = impactor stage cut diameter, μmA
μ_G = gas viscosity, poise
d_j = jet diameter, cm
u_j = jet velocity, cm/s

The particle diameter used is called "aerodynamic diameter" and it has the unit of "aerodynamic microns," μmA. This is the effective diameter for particle separation by inertial impaction and it takes into account the effects of particle density and particle "slip" between gas molecules. It is related to the actual physical size of the particle by the following equation:

$$d_{pa} = d_p \sqrt{\rho_p \, C'} \tag{8}$$

where: d_{pa} = aerodynamic particle diameter, μmA
d_p = actual particle diameter, μm
ρ_p = particle density, g/cm³
C' = Cunningham slip correction factor, dimensionless

At room temperature for air the Cunningham slip correction factor, C', is given by:

$$C' = 1 + \frac{0.165}{d_p} \tag{9}$$

If the particle distribution follows the log-normal law, a straight line will result on log-probability paper. The 50% value of particle diameter is the geometric mass mean diameter, d_{pg}, and the geometric standard deviation, σ_g, is given by:

$$\sigma_g = \frac{84.3\% \text{ value of } d_{pa}}{50\% \text{ value of } d_{pa}} \tag{10}$$

Overall Particle Penetration

Overall particle penetration is defined as:

$$\overline{Pt} = \frac{1}{C_{pti}} \int_0^\infty Pt(d_p)\ f(d_p)\ \bar{d}\ d_p \qquad (11)$$

$$= \frac{\text{mass concentration out}}{\text{mass concentration in}}$$

where: $\overline{Pt}$ = overall particle penetration, fraction

$Pt(d_p)$ = penetration for particles with diameter d_p, fraction

$f(d_p)$ = particle frequency distribution

C_{pti} = total inlet particle concentration, mg/DNm^3

The overall particle penetration can be computed using the data from a simulatneous inlet and outlet cascade impactor or filter run.

Particle Penetration as a Function of Particle Diameter

The particle penetration for particle diameter, d_{pi}, or grade penetration curve is given by:

$$Pt(d_p) = \frac{\left[\frac{\bar{d}C_p}{\bar{d}(d_p)}\right]_{\text{outlet}}}{\left[\frac{\bar{d}C_p}{\bar{d}(d_p)}\right]_{\text{inlet}}} \qquad (12)$$

where: $\frac{\bar{d}C_p}{\bar{d}(d_p)}$ = the slope of the cumulative mass concentration versus particle diameter curve at d_p, mg/DNm^3 - μmA

Particle penetration as a function of particle size is computed from inlet and outlet particle size distributions and concentration data. The major steps involved in the computation are as follows:

1. Reduce cascade impactor data to the form of cumulative particle mass concentration for each impactor cut diameter.

2. Determine the slopes of the cumulative mass distribution curves at several values of particle diameter for both the inlet and outlet and then compute penetration at each particle diameter.

There are several techniques to determine the slope of the cumulative mass distribution curve. Some of the techniques are discussed below.

1. Graphical technique - Cumulative mass concentration versus aerodynamic particle diameter data may be fitted with a curve by eyeball method. The slopes of the curve at various values of particle diameter are then measured graphically.

2. Curve fitting - Curve fitting to the data points and the measurement of curve slopes by eye involves subjective judgment. To eliminate the judgment errors, it is possible to fit the data with a mathematical function and then evaluate the slope analytically. We have tried fitting the cumulative mass curves to log-normal distribution functions, and the Weibull distribution.

Log-normal Distribution -

If the inlet and outlet size distributions are nearly log-normal, then a purely mathematical particle penetration is used. This mathematical log-normal penetration is based on the following:

The cumulative distribution of particle sizes is:

$$P(x) = \frac{1}{(2\pi)^{\frac{1}{2}}} \int_{-\infty}^{x} e^{-t^2/2} dt \qquad (13)$$

where $P(x)$ is the cumulative mass fraction of sizes smaller than "d_{pa}", and

$$x = \frac{\ln d_{pa} - \ln d_{pg}}{\ln \sigma_g} \qquad (14)$$

The derivative of the distribution function is:

$$\frac{\bar{d}\ P}{\bar{d}\ d_{pa}} = \frac{\bar{d}\ P}{\bar{d}\ x}\ \frac{\bar{d}\ x}{\bar{d}\ d_{pa}} = \frac{\exp\ (-x^2/2)}{(2\pi)^{\frac{1}{2}}\ d_{pa}\ \ln\ \sigma_g} \qquad (15)$$

thus,

$$\frac{\bar{d}\ C_p}{\bar{d}\ d_{pa}} = \frac{C_{pt}\ \exp(-x^2/2)}{(2\pi)^{\frac{1}{2}}\ d_{pa}\ \ln\ \sigma_g} \qquad (16)$$

Using equation (12), the penetration is then:

$$Pt = \frac{C_{pto}}{C_{pti}}\ \frac{(\ln\ \sigma_g)_{in}}{(\ln\ \sigma_g)_{out}}\ \exp\left(\frac{x^2\ in\ -\ x^2\ out}{2}\right) \qquad (17)$$

Weibull Distribution -

The Weibull distribution, Lipson and Sheth (1973), offers two advantages over the log-probability distribution. The first is that it has three parameters rather than two. The second is that the cumulative distribution function (CDF) is explicit and does not have to be approximated by multi-termed polynomials.

Cumulative distribution function -

$$CDF = 1 - \exp\left[-\left(\frac{d_p - d_{po}}{\Theta - d_{po}}\right)^b\right] \qquad (18)$$

where d_p = particle diameter, cm
d_{po} = minimum particle diameter, cm
Θ = characteristic diameter, cm
b = Weibull slope, dimensionless

The CDF has the property that:

$$\text{CDF}\ (\Theta = d_p) = 0.632 \tag{19}$$

The median particle diameter occurs when the CDF = 0.5, so:

$$d_{pm} = d_{po} + (\Theta - d_{po})\ (\ln 2)^{1/b} \tag{20}$$

Linear transformation - Transformation to a linear form:

$$y = A + B\,x \tag{21}$$

requires that:

$$y = \ln\left[\ln\left(\frac{1}{1-\text{CDF}}\right)\right] \tag{22}$$

$$x = \ln\,(d_p - d_{po}) \tag{23}$$

therefore,

$$A = -b\ \ln\,(\Theta - d_{po}) \tag{24}$$

$$B = b$$

and,

$$\Theta = d_{po} + \exp\left(-\frac{A}{B}\right) \tag{25}$$

$$b = B$$

Least squares curve fit - The minimum particle diameter, d_{po}, is that which results in the highest linear correlation coefficient based on the above linear transformation, when a least squares linear regression is performed on the size distribution data. Note that,

$$0 \leq d_{po} < \text{smallest diameter found in the distribution}$$

Density function - The Weibull density function is the derivative of the CDF:

$$f(d_p) = \frac{b}{\Theta - d_{po}} \left(\frac{d_p - d_{po}}{\Theta - d_{po}} \right)^{b-1} \exp \left[- \left(\frac{d_p - d_{po}}{\Theta - d_{po}} \right)^{b} \right] \qquad (26)$$

Penetration - The penetration is the ratio of the cumulative mass loading distribution derivatives,

$$Pt\ (d_p) = \frac{C_{pto}\ f_{out}\ (d_p)}{C_{pti}\ f_{in}\ (d_p)} \qquad (27)$$

where: C_{pt} = total mass concentration or loading, mg/DNm^3
"o" or "out" = refers to outlet particle size distribution
"i" or "in" = refers to inlet particle size distribution
and $f(d_p)$ = is defined above.

Minimum particle diameter, physical interpretation - "d_{po}" is the smallest diameter of the total distribution. A value other than zero means that the data indicate that there is a minimum particle size. This is physically reasonable because of the particle formation mechanisms and possible agglomeration and/or particle growth.

Characteristic diameter, physical interpretation - "Θ" is analogous to the geometric mean particle diameter of the log-probability distribution and is therefore an indication of the

"average" size of the particles in the distribution. The median particle diameter is directly related to "Θ" by equation (20).

Weibull slope, physical interpretation - "b" is analogous to the geometric standard deviation of the log-probability distribution. It indicates the "spread" of the size distribution. The larger the Weibull slope, b, the more uniform (monodisperse) the particle sizes.

SCREEN DIFFUSION BATTERY DATA ANALYSIS

Screen diffusion battery data consist of particle number concentrations which are obtained after each stage in the diffusion battery. Particle penetrations are calculated from the ratio of the number concentration taken at a given SDB stage to the inlet number concentration. The particle size distribution may then be determined from the penetration data.

Most particle formation processes result in a particle size distribution which is log-normal. Log-normal size distributions are conveniently represented by two parameters: the number geometric mean diameter (d_{pn}) and the standard deviation (σ_g). Typically, process created aerosols fail log-normality only at the extremes of large and small particles which represent only a small percentage of the total particulates.

Calvert, et al. (1972) describe a method for converting log-normal size distributions to overall penetrations using the relation between particles of a discrete diameter, and penetration of those particles through the device.

The equation is a discrete form of the following equation:

$$\overline{Pt} = \int_{-\infty}^{\infty} Pt\ f(d_p)\ \bar{d}(\ln d_p) \qquad (28)$$

where, for a screen diffusion battery:

$$Pt = \exp\ (-A\ S\ d_p^{\ B}) \qquad (29)$$

and, Pt = penetration fraction of a particle of a given diameter through S

S = solidity factor, a dimensionless parameter

d_p = particle diameter, μm

A,B = constants established by theory and laboratory experimentation, dimensionless

and for a log-normal distribution:

$$f(d_p) = \frac{1}{\sqrt{2\pi}\ \ln \sigma_g} \exp\left[- \left(\frac{\ln d_p - \ln d_{pn}}{\sqrt{2\pi}\ \ln \sigma_g} \right)^2 \right] \qquad (30)$$

Calvert and Patterson (1977) have shown that for particles in the size range of 10^{-3} μm < d_p < 10^{-1} μm the penetration through the SDB is given by:

$$Pt = \exp\left[-1 \times 10^{-4}\ S\ (u_s\ d_c)^{-0.67} d_p^{-1.29} \right] \qquad (31)$$

where: u_s = superficial gas velocity, cm/s

d_c = wire diameter of screen, cm

Thus, the variables in equation (29) have the following values:

$$A = 1 \times 10^{-4}\ (u_s\ d_c)^{-0.67}$$

$$B = -1.29$$

The particle diameter that penetrates a SDB stage with 50% efficiency is found by substituting 0.5 for Pt in equation (29):

$$d_{pc} = \left[\frac{-\ln (0.5)}{AS} \right]^{1/B} \qquad (32)$$

Each stage will have a certain "d_{pc}" for a given flow rate.

In order to determine the number geometric mean diameter, d_{pn}, and standard deviation, σ_g, of the particles entering the SDB a curve matching technique must be used. The data consist of overall penetration, Pt (ratio of outlet to inlet particle concentration), and stage cut diameter, d_{pc}, for each screen. A plot of these data points must match a curve that is a numerical solution to equation (28) such as one of those presented by Calvert, et al. (1972). The curve most closely matched will determine the "d_{pn}" and "σ_g" of the particles entering the SDB.

Non-log normal data must be handled by a graph stripping technique outlined by Sinclair (1972) which entails tedious graphical integration and mathematical conversions. In our experience the data have fallen sufficiently close to log-normality that the curve matching technique is acceptable.

Conversion of number distribution to mass distribution is necessary in order to put the diffusion battery and cascade impactor data on the same basis. The method used to make this conversion is a graphical integration of the following equation:

$$C_{pi} = \frac{N_{pt}}{100} \int_0^{N_{pi}} \frac{\bar{d}m_p}{\bar{d}N_p} \, \bar{d}\left(\frac{N_p \times 100}{N_{pt}}\right) \qquad (33)$$

where: N_p = cumulative number concentration of particles smaller than "d_p", #/cm^3

N_{pt} = total number concentration of particles, #/cm^3

d_p = particle diameter, μm

d_{pi} = mass of particles in the infinitesimal size range $(d_p + \bar{d}d_p)$, g

C_{pi} = cumulative mass concentration of particles smaller than "d_{pi}", g/cm^3

The quantity (dm_p/dN_p) is simply the mass per particle of diameter "d_p". The quantity ($N_p \times 100/N_{pt}$) is the number percent of particles smaller than "d_p". Thus, equation (33) can be evaluated from a plot of mass per particle versus cumulative number percent of particles, both quantities being evaluated at the same particle diameter to provide a point on the plot. The total and cumulative number concentration data are obtained as described previously.

For a log-normal distribution the mass and number distribution are related by:

$$\sigma_g \text{ (number)} = \sigma_g \text{ (mass)} \tag{34}$$

$$\ln d_{pg} = \ln d_{pn} + 3 \ln^2 \sigma_g \tag{35}$$

Finally, since impactor data are usually reported as mass aerodynamic impaction diameters, equation (8) must also be used to complete the comparison of SDB and cascade impactor data.

REFERENCES

Calvert, S., J. Goldshmid, D. Leith, and D. Metha, "Scrubber Handbook" NTIS PB 213-016, 1972.

Calvert, S. "Engineering Design of Fine Particle Scrubbers", J. of APCA. 24: 929, 1974.

Calvert, S., C. Lake, and R. Parker "Cascade Impactor Calibration Guidelines" EPA-600/2-76-118, 1976a.

Calvert, S., H.F. Barbarika, and C.F. Lake "National Dust Collector Model 850 Variable Rod Module Venturi Scrubber Evaluation" EPA-600/2-76-282, 1976b.

Calvert, S., H.F. Barbarika, and G.M. Monahan "Gas Atomized Spray Scrubber Evaluation" EPA-600/2-77-209a, 1977a.

Calvert, S., H.F. Barbarika, and G.M. Monahan "American Air Filter Venturi Evaluation" EPA 600/2-77-209b, 1977b.

Calvert, S. and R.G. Patterson "Submicron Particle Size Measurement with a Screen Diffusion Battery", Final Report, EPRI Contract RP 723-1-760205, 1977.

Fegley, M.J., D.S. Ensor, and L.E. Sparks "The Propagation of Errors in Particle Size Distribution Measurements Performed Using Cascade Impactors" Paper 75-32.5 presented at the 68th Annual Meeting of APCA, Boston, MA, June 15-20, 1975.

Harris, D.B. "Procedures for Cascade Impactor Calibration and Operation in Process Streams" EPA 600/2-77-004, January 1977.

Lipson, C. and N.J. Sheth "Statistical Design and Analysis of Engineering Experiments", McGraw-Hill, 1973.

Lundgren, D.A. "An Aerosol Sampler for Determination of Particle Concentration as a Function of Size and Time", J. of APCA, 17: 225, 1967.

Rao, A.K. "Sampling and Analysis of Atmospheric Aerosols", Particle Technology Laboratory, Mechanical Technology Laboratory, University of Minnesota. Publication 269, 1975.

REFERENCES (continued)

Sinclair, D. "A Portable Diffusion Battery" American Ind. Hygiene Assoc. Journal 33: 729-735, 1972.

Smith, W.B., K.W. Cushing, and J.D. McCain "Particle Sizing Techniques for Control Device Evaluations" EPA 650/2-74-102, NTIS PB 240670/AS, October 1974.

Sparks, L.E. Personal Communication, 1971.

Yung, S., S. Calvert and H.F. Barbarika "Venturi Scrubber Performance Model" EPA-600/2-77-172, 1977a.

Yung, S., H.F. Barbarika and S. Calvert "Pressure Loss in Venturi Scrubbers" J. Air Poll. Control Assoc., 27: 348-351, 1977b.

TECHNICAL REPORT DATA
(Please read Instructions on the reverse before completing)

1. REPORT NO.	2.	3. RECIPIENT'S ACCESSION NO.
EPA-600/2-78-032		

4. TITLE AND SUBTITLE	5. REPORT DATE
Evaluation of Three Industrial Particulate Scrubbers	February 1978
	6. PERFORMING ORGANIZATION CODE

7. AUTHOR(S)	8. PERFORMING ORGANIZATION REPORT NO.
Seymour Calvert, Harry F. Barbarika, and Gary M. Monahan	

9. PERFORMING ORGANIZATION NAME AND ADDRESS	10. PROGRAM ELEMENT NO.
Air Pollution Technology, Inc. 4901 Morena Boulevard, Suite 402 San Diego, California 92117	1AB012; ROAP 21ADM-029
	11. CONTRACT/GRANT NO.
	68-02-1869

12. SPONSORING AGENCY NAME AND ADDRESS	13. TYPE OF REPORT AND PERIOD COVERED
EPA, Office of Research and Development Industrial Environmental Research Laboratory Research Triangle Park, NC 27711	Final; 3/75-12/77
	14. SPONSORING AGENCY CODE
	EPA/600/13

15. SUPPLEMENTARY NOTES IERL-RTP project officer is Dale L. Harmon, Mail Drop 61, 919/514-2925. Earlier reports in this series are EPA-600/2-76-282 and EPA-600/2-77-209a and -209b.

16. ABSTRACT

The report gives results of field measurements, carried out on three full scale industrial scrubbers to determine scrubber performance characteristics, including particle collection efficiency as a function of particle diameter. The three scrubbers were different gas-atomized spray types with pressure drops ranging from 54 to 178 cm W.C. Their performance on major sources of fine particle emissions was compared to a mathematical performance model for venturi scrubbers.

17. KEY WORDS AND DOCUMENT ANALYSIS

a. DESCRIPTORS	b. IDENTIFIERS/OPEN ENDED TERMS	c. COSATI Field/Group
Pollution Dust Scrubbers Industrial Processes Measurement Gases Atomizing Spraying	Pollution Control Stationary Sources Particulate Collection Efficiency	13B 11G 07A 13H 14B 07D

18. DISTRIBUTION STATEMENT	19. SECURITY CLASS *(This Report)*	21. NO. OF PAGES
Unlimited	Unclassified	99
	20. SECURITY CLASS *(This page)*	22. PRICE
	Unclassified	

EPA Form 2220-1 (9-73)